ADDIS ABABA UNIVERSITY

ADDIS ABABA INSTITUTE OF TECHNOLOGY

SCHOOL OF CIVIL AND ENVIRONMENTAL ENGINEERING

PARAMETRIC STUDY ON STABILITY ANALYSIS OF A THIN SHELL STRUCTURE UNDER OWN WEIGHT

A Thesis in Structural Engineering

By Tamirat Kebede

May 2020

Addis Ababa

A Thesis

Submitted in Partial Fulfillment of the Requirements for the Degree of Master of Science

The undersigned have examined the thesis entitled '**Parametric Study on Stability Analysis of a Thin Shell Structure under Own Weight**' presented by **Tamirat Kebede**, a candidate for the degree of **Master of Science** and hereby certify that it is worthy of acceptance.

Dr. Shifferaw Taye		
Advisor	Signature	Date
Internal Examiner	Signature	Date
External Examiner	Signature	Date
Chairperson	Signature	Date

UNDERTAKING

I certify that research work titled "**Parametric Study on Stability Analysis of a Thin Shell Structure under Own Weight**" is my own work. The work has not been presented elsewhere for assessment. Where material has been used from other sources it has been properly acknowledged/referred.

Tamirat Kebede

ABSTRACT

Paraboloid shells are translational shells formed from two parabolas placed at the right angle to each other and by the translation of one parabola over the other. Elliptical paraboloid is formed by two unequal parabolas with the same curvature sign.

Thin concrete elliptic paraboloid shell with large spans are susceptible to buckling. Determining the critical buckling load, internal forces and free vibration is difficult because of the lack of experimental study on such shell type.

The research is focused on the analysis of an elliptic paraboloid shell structure under its own weight. Geometrical and material linearity are considered in modeling and analysis of the structure in this study. The objective of the research is the parametric study on stability analysis of a thin shell structure under its own weight.

In this study, the internal forces, moments, deformation, stability, and free vibration of elliptic parabolic shell analysis are performed by theoretical and finite element methods. Theoretical analysis is done by shallow shell theory and the finite element analysis is carried out by using DLUBAL RFEM 5.3.1.

Theoretical formulas in this study are coded by the MATLAB program. The codes are used to determine internal force, moments, in-plane shear, displacement, critical load and time, angular frequency, natural frequency in free vibration are written in the appendix.

The influences of the different parameters on the critical loads of the shells are thereby studied. The parameter considered is thickness, the radius of curvature, modulus of elasticity and side rise of the shell to determine the critical buckling load. Free vibration analysis of rectangular and square planned elliptic paraboloid shell structures was done.

Finally, the internal forces, displacement, critical buckling load, and free vibration analysis result in the study presented graphically and discussed in detail. The result of the finite element analysis is then compared with the theoretical analysis results.

ACKNOWLEDGMENTS

First, I would like to thank God that help me throughout all the process of this research. Then, I would also like to acknowledge Dr. Shifferaw Taye of the civil and environmental engineering at Addis Ababa institute of technology as the second reader of this thesis, and I am gratefully indebted to his for his very valuable comments on this thesis.

Finally, I must express my very profound gratitude to my parents and my wife for providing me with unfailing support and continuous encouragement throughout my years of study and through the process of researching and writing this thesis. This accomplishment would not have been possible without them. Thank you.

TABLE OF CONTENTS

LIST OF TABLES

LIST OF FIGURES

CHAPTER 1 INTRODUCTION

1.1 Background

Reinforced concrete thin shells can be defined as curved slabs whose thicknesses are small compared to their other dimensions like the radius of curvature. Due to its initial curvature, a shell can transfer an applied load by in-plane as well as out-of-plane actions. A thin shell subjected to an applied load, therefore, produces mainly in-plane actions, which are called membrane forces. These membrane forces are resultants of normal stresses and in-plane shear stresses that are uniformly distributed across the thickness.

Shell structures can be efficiently and economically used in various fields of engineering and architecture. Examples of shell structures in civil and architectural engineering are large-span roofs, liquid-retaining structures, and water tanks, containment shells of nuclear power plants, and concrete arch domes.

Deformable bodies may become unstable under certain loading conditions and thus have a premature failure. The phenomenon of instability is particularly important for thin shells subjected to compressive forces.

Elliptic paraboloid shell is a doubly curved, synclastic, and non-developable surface. Therefore, it is generally very strong and highly stable. The critical stability load of the elliptic paraboloid shell is usually much higher than those of concrete shells with single curvature. Nevertheless, thin concrete elliptic paraboloid with a large span is susceptible to buckling; indeed the buckling consideration is one of the main design criteria of such shell.

1.2 Statement of the Problem

It is thus seen that though, the critical buckling load and free vibration of cylindrical and some other shells were studied extensively by many researchers, very less work were carried out on the buckling and free vibration characteristics of doubly curved shells. The study of buckling and free vibration behavior of doubly curved elliptic paraboloid, hyperbolic paraboloid, conidial and hypar shells is yet to be carried out. The present work

is, therefore, expected to investigate the critical buckling and the free vibration behavior of the elliptic paraboloid shell by employing the theoretical and finite element method.

1.3 Significance of the Research

The significance of this thesis is to understand the impact of the self-weight of elliptical paraboloid thin shell parameters on buckling and natural vibration. The purpose of this study is to determine the impact of variable parameters on the reinforced concrete elliptic paraboloid shell. RFEM software is used for modeling elliptic paraboloid shell so that other researchers can refer and use it for modeling other shell structures.

1.4 The Objective of the Research

1.4.1 General Objective

The main objective of this research is to perform a parametric study on stability analysis of a thin shell structure under its own weight by using theoretical and finite element analysis methods.

1.4.2 Specific Objective

- Determine the critical buckling load of the shell under its own weight.
- To determine the effect of varying parameters on the critical buckling load on the elliptic paraboloid shell structure.
- To calculate and compare the internal forces, moment, deflection, buckling load, and natural vibration on the shell structure by theoretical and finite element analysis.
- To visualize the buckling and natural vibration mode shape by RFEM finite element program.

1.5 Scope of the Research

This research is limited to the consideration in some intervals of parameters it may not work for other values outside the considered parameters of thin elliptic paraboloid shells.

This study also restricted to elliptic paraboloid reinforced concrete shell under geometrical and material linearity.

1.6 Organization of the Thesis

This thesis is categorized into five chapters and prepared as follows.

Chapter One The introduction and general background of the study, statement of the problem, significance, scope, and objectives of the research.

Chapter Two More tells about the literature review and basic definitions and theories about shell structures. A review of literature that includes the reviews of selected previous works on the elliptic paraboloid shell. In this chapter also the concept of stability and instability discussed.

Chapter Three Explain the materials, analysis methods, and the finite element programs that were used in the study. This chapter also contains some sample solved elliptic paraboloid shell by different theoretical equations and the procedures to be followed for modeling and analyzing the structure by the finite element program.

Chapter Four Based on the theoretical equations, material, analysis method, and finite element program presented in chapters 2 and 3, the study presented in this chapter has mainly expressed the results obtained by different analyses methods and discuss on its.

Chapter Five The conclusions of the research based on the results and recommendations on future researches.

CHAPTER 2 LITERATURE REVIEW

2.1 General

This literature review generally focused on the related research of a parametric study on stability analysis of a thin reinforced concrete shell structure. A review of some of the previous studies on the stability analysis of the elliptic paraboloid shell is presented in this section.

S.N. Krivoshapko and G.L. Gbaguidi-Aisse [1] have reviewed geometry, static, vibration, and buckling analysis and applications to thin elliptic paraboloid shells. Their review work attempts to organize and summarized the extensive published literature on the basic achievements in investigations of thin-walled structures in the form of elliptic paraboloids. Geometrical researches, approximation, and bending of elliptic paraboloid surfaces, research of the stress-strain state of shells by theoretical and numerical methods, natural and forced vibration of a shell, forming and setting of surfaces, application of shells in the form of elliptic paraboloids are the main problems which are considered in their review.

Generally, they tried to assemble various research on this commonly used form of the thin elliptic paraboloid shell structure.

Elastic analysis of the elliptic paraboloid shell is studied by A. M. Ansah [2]. His research investigated a general solution for elliptic paraboloids, valid for any set of boundary conditions that maintain or tend to maintain the four corners of the shell in fixed positions in space, is presented together with some numerical results. From his study, he concludes that elliptic paraboloid is essentially characterized by direct compression stresses and that bending stresses are relatively small, except in free-edge shells.

D. Hamadi, R. Chebili, and M. Mellas [3] performed research on a numerical and experimental investigation of an elliptical paraboloid shell model. They formulated an element that can be used for the analysis of thin shell structures; no matter how the geometrical shape might be. Tests on standard problems have been examined. Since the analysis of thin shells, structures have generally been purely carried out on a theoretical basis. They also offered some experimental results of an elliptical paraboloid under

uniformly distributed load pressure. The results obtained from both numerical and experimental work are presented on their research.

T. Nagay [4] investigated on some problems of the numerical analysis of elliptic paraboloid shallow shells. He executed flexural and membrane stresses of the mid-point of a shell 10 by 10 m in-ground plan and 10 cm thick and plotted linear and nonlinear theoretical results. He also determined the critical load by iteration of geometric energetical procedures.

Bending analysis of the paraboloid of the revolution shell is studied by N. Tamboli and A.B. Kulkarni [5]. In the study, they attempt to analyze the paraboloid of revolution for bending using the finite element method. A Vlasov bending theory is used to solve the bending analysis theoretically. From the results obtained they concluded that the results of STAAD. Pro software and theoretical analysis for paraboloid of revolution have more or less good agreement in the stresses.

B. Mohraz and W.C Schnobrich [6] explored the analysis of shallow shell structures by a discrete element system. They develop the discrete model to analyze and obtain numerical results of simply supported and uniformly loaded elliptic parabolic shells and plotted diagrammatically. They also examined uniformly and sinusoidally varying loaded and rectangular plate, cylindrical shell, hyperbolic paraboloid, and hyperbolic paraboloid bounded by characteristics lines of the surface.

The work of S. Kato, Y. Yamauchi, T. Ueki, and K. Okuhira [7] are focused on the critical buckling load of simply supported rectangular plan elliptic paraboloid single-layer reticulated roof under uniform load. The buckling analyses were done for linear buckling, elastic buckling, and elastic-plastic buckling. Based on the theoretical results, a procedure to estimate elastic-plastic buckling loads were presented on their work. They used the procedure is based on a concept for column buckling strength in terms of generalized slenderness ratio considering shell-like behavior, and it was proved to give a reasonable estimation for elastic and elastic-plastic buckling loads for elliptic paraboloidal roofs under a uniform load.

Researchers F. Ruo-Qiang, Y. Jihong, and Y. Bin has studied the evaluation of buckling load of an elliptic paraboloid cable braced grid shell by using the continuum analogy. They

derived the formula from the continuum analogy and verified with numerical examples [8].

Buckling strength of stiffened elliptic paraboloidal steel panels was performed by A. Zingoni and V. Balden [9] and the results of a numerical study undertaken on the buckling behavior of lightly stiffened elliptic paraboloidal steel panels intended for use as long-span shuttering for lightweight concrete bridge decks, walkways, and floors. The results concluded that the panel rise and aspect ratio have a considerable influence on the buckling strength of the shutter.

N.N. Meleka, M.A. Safan, A.A. Bashandy, A.S. Abd-Elrazek [10] is carried out to evaluate the repair and strengthening of the techniques of elliptical paraboloid reinforced concrete shells with openings. They strengthen the shell by glass fiber reinforced polymers GFRP at different positions of the shell bottom surface, steel strip, and external tie.

A. Bryan [11] is investigated on the free vibration of thin shallow elliptical shells and he got the results of examples to demonstrate that the eigenfrequencies of thin shallow elliptical shells are directly proportional to the curvature of the shell and inversely proportional to the shell's eccentricity.

A. N. Nayak and J. N. Bandyopadhyay [12] carried out on the free vibration of stiffened shallow shells. They presented the finite element analysis results for free vibration behavior of doubly curved stiffened shallow shells.

2.2 Definitions and Fundamentals of Shells

The term shell is applied to bodies bounded by two curved surfaces, where the distance between the surfaces is small in comparison with other body dimensions [13].

Shells are spatially curved surface structures that support externally applied loads. Shells are found in a variety of natural structures such as eggs, plants, leaves, skeletal bones, and geological forms. Shell structures have also been built by man since the most ancient times. Many shell domes built of masonry and stone in ancient times are still in existence in some parts of the world.

The locus of points that lie at equal distances from these two curved surfaces defines the middle surface of the shell. The length of the segment, which is perpendicular to the curved surfaces, is called the thickness of the shell and is denoted by *h*. The geometry of a shell is entirely defined by specifying the form of the middle surface and thickness of the shell at each point.

A thin shell has a very small thickness-to-minimal-radius ratio, often smaller than 1/50. As with plates, an applied load that acts out-of-plane leads to larger displacements than those generated by a load acting in-plane with the same intensity. Due to its initial curvature, a shell can transfer an applied load by in-plane as well as out-of-plane actions. A thin shell subjected to an applied load, therefore, produces mainly in-plane actions, which are called membrane forces. These membrane forces are resultants of normal stresses and in-plane shear stresses that are uniformly distributed across the thickness.

Reinforced concrete thin shells can be defined as curved slabs whose thicknesses are small compared to their other dimensions like the radius of curvature. Even though shell construction with steel and concrete is used in the industry for pressure vessels, reactors, etc.

There are two different classes of shells: thick shells and thin shells. A shell is called thin if the maximum value of the ratio *h*/*R* (where *R* is the radius of curvature of the middle surface) can be neglected in comparison with unity. For an engineering accuracy, a shell may be regarded as thin if the following condition is satisfied:

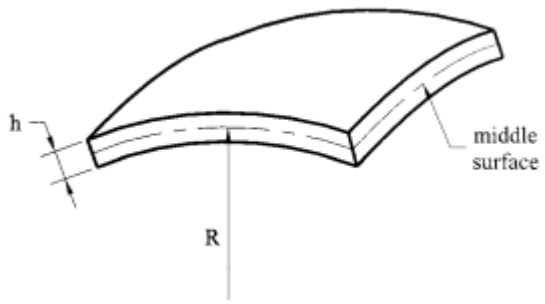

Figure 2-1: Shell dimension

$$\text{Max}\left(\frac{h}{R}\right) \leq \frac{1}{20}$$

Hence, shells for which this inequality is violated are referred to as thick shells. For a large number of practical applications, the thickness of shells lies in the range i.e., in the range of thin shells.

$$\frac{1}{1000} \leq \frac{h}{R} \leq \frac{1}{20}$$

2.3 Uses of Shell Structures

Shell structures can be efficiently and economically used in various fields of engineering and architecture. Examples of shell structures in civil and architectural engineering are large-span roofs, liquid-retaining structures, and water tanks, containment shells of nuclear power plants, and concrete arch domes [13].

Recently, with the advent of various fiber-reinforced and laminated composite materials, the domain of application and range of structural efficiency of shell forms has immensely increased.

The wide application of shell structures in engineering is conditioned by the following advantages:

1. The efficiency of load-carrying behavior.
2. The high degree of reserved strength and structural integrity.
3. High strength: weight ratio. This criterion is commonly used to estimate a structural component efficiency: the larger this ratio, the more optimal is a structure. According to this criterion, shell structures are much superior to other structural systems having the same span and overall dimensions.
4. Very high stiffness.
5. Containment of space.

2.4 Classification of Shells

2.4.1 Based On Gaussian Curvature of a Surface

The geometry of a shell is completely described by the curved shape of the middle surface and the thickness distribution of the shell [13]. At any point A on a smooth surface, there

is a tangent plane. The normal to the surface at that point is defined to be normal to the tangent plane, as shown in figure 2-2. A plane through point *A* that contains the normal is said to be normal to the middle surface at *A*. The intersections of the normal planes and the middle surface normal sections of the surface at *A*. Each of these curves has a local curvature *K* and a corresponding radius of curvature *R*. If the origin of the radius is at the positive side of the normal to the surface, the relation between the radius and the curvature is $R = K$. If the origin is at the negative side of the normal, the relation is $R = -K$.

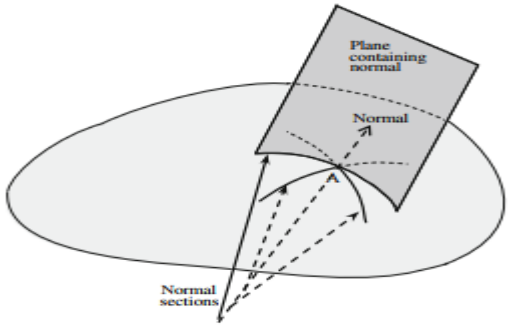

Figure 2-2: Intersection of a plane with a surface

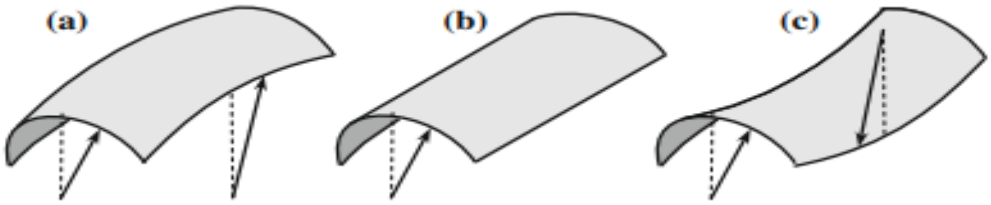

Figure 2-3: Gaussian curvature

(a) Positive Gaussian curvature. (b) Zero Gaussian curvature. (c) Negative Gaussian curvature

The product of the two principal curvatures $\Gamma = K_1 \times K_2$ is called the Gaussian curvature of the surface at *A*. The Gaussian curvature can be positive, negative, or zero. If it is positive, so that K_1 and K_2 have the same sign, the surface is said to be synclastic at that point. If it is negative, so that K_1 and K_2 have opposite signs, it is said to be anticlastic. If it is zero, one or both of K_1 and K_2 are zero. The surface is said to have a single curvature.

2.4.2 Classification Based On Geometrical Developability

2.4.2.1 Developed and Undeveloped Surfaces

A surface is said to be developable if it can be deformed into plane form without cutting or stretching its middle surface. A surface that cannot be deformed into plane form in this way is said to be undevelopable. Both cases are shown in figure 2-4. Surfaces with double curvature cannot be developed, while those with single curvature can be developed. In other words, surfaces with positive or negative Gaussian curvature (i.e. synclastic and anticlastic surfaces) cannot be developed, while those with zero Gaussian curvature can be developed. Developability and undevelopability are geometrical properties of a surface, but they have structural significance. Shells that cannot be developed require more external energy to be deformed (i.e. to be stretched out, to be bent, to be destructed) than developable shells. Shells that cannot be developed are, in general, stronger and more stable than shells that can be developed having the same overall dimensions.

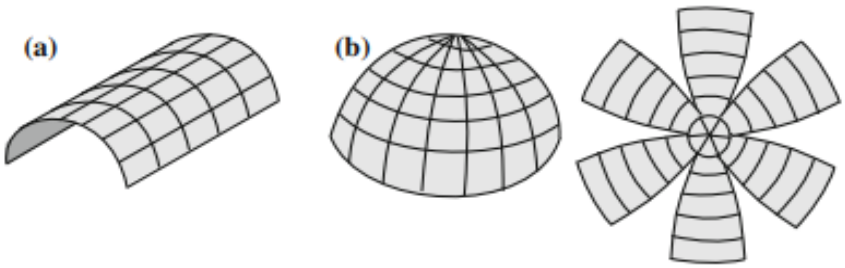

Figure 2-4: Examples of a shell surface

(a) A surface that can be developed. (b) A surface that cannot be developed.

2.4.3 Classification Based On Geometric Form

Based on geometric form there are four types of shell categories but this research mainly focused and discussed on the surface of translation shells, that is an elliptic paraboloid shell.

2.4.3.1 Surfaces of translation

A surface of translation is defined as the surface generated by keeping a plane curve parallel to its initial plane as it has moved it along another plane curve. The two planes containing the two curves are at right angles to each other. An elliptic paraboloid is shown

in figure 2-5 as an example of such a type of surface. It is obtained by translation of a parabola on another parabola; both parabolas have their curvatures in the same direction. Therefore, this shell has a positive Gaussian curvature. For this surface sections, x = constant and y = constant are parabolas, whereas a section z = constant represents an ellipse: hence its name, ‘‘elliptic paraboloid.’’

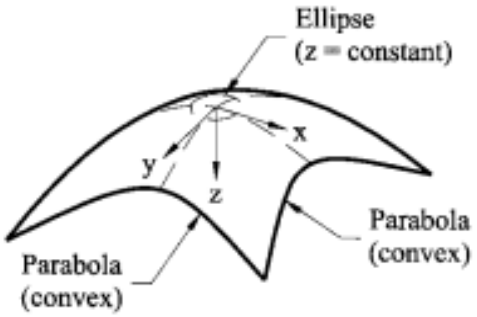

Figure 2-5: Example of the surface of the translation shell

2.5 Paraboloid Shells

In his book, P.C Varghese [14] explains the design of paraboloid shells. In the book paraboloid shells defined and classified as follows. Paraboloid shells are translational shells formed from two parabolas placed at the right angle to each other and by the translation of one parabola over the other. The common paraboloids may be subdivided into the following three groups:

1. Elliptical paraboloid. This type is formed by two unequal parabolas with the same curvature sign (both convex curved in the same direction).
2. Circular paraboloid. This type is formed by two equal parabolas with the same curvature sign (both concave curved in the same direction).
3. Hyperbolic paraboloid. This type is formed by two parabolas of opposite curvatures (one convex and the other concave curved in the opposite directions).

Table 2-1: Types of shells formed by parabolic directrix

Directrix	Generator	Horizontal Section	Name of Surface
Concave Parabola	Straight Line	Straight Line	Parabolic cylinder
Convex parabola	Unequal Convex Parabola	Ellipse	Elliptical Paraboloid
Convex parabola	Equal Convex Parabola	Circle	Circular Paraboloid
Convex parabola	Concave Parabola	Paraboloid	Hyperbolic Paraboloid

2.6 Shallow Shell

Shallow shell and shallow shell theory must be stated and reflected because it integrated corporately with the membrane analysis of the shell. Shallow shell is briefly and explained in thin plates and shells theory, analysis, and application book [15].

A shallow shell is defined as a shell having a relatively small raise as compared to its spans. A shell is said to be shallow if at any point of its middle surface the following inequalities hold:

$$\left(\frac{dz}{dx}\right)^2 \approx 1, \qquad \left(\frac{dz}{dy}\right)^2 \approx 1 \tag{2-1}$$

where $z = z\ (x, y)$ represents the equation of the shell middle surface. Referring to figure 2-6, one sees the effect of this simplification. Consider a differential element of the middle surface bounded by the intersections with two planes parallel to the *Oyz* coordinate plane and separated by a distance *dx*, and two planes parallel to the *Oxz* coordinate plane separated by a distance *dy*. From figure 2-6, it follows that

$$ds_1 \cong dx\left[1+\left(z,x\right)^2\right]^{1/2} \tag{2-2}$$

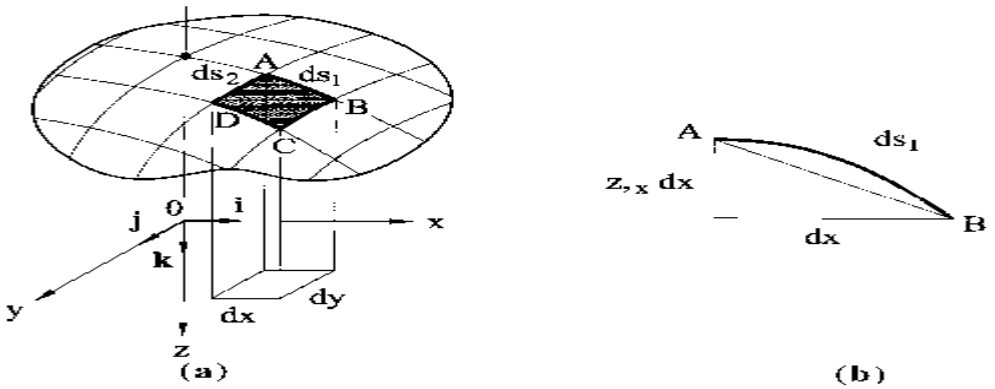

Figure 2-6: Differential element of a shell

Similarly, it can be written

$$ds_2 \cong dy\left[1+\left(z,y\right)^2\right]^{1/2} \qquad 2\text{-}3$$

These expressions, due to the geometric simplification equation 2.2 and 2.3, may be written simply as

$$ds_2 \approx dy \quad and \quad ds_1 \approx dx \qquad 2\text{-}4$$

Practically, the above implies that the curvilinear coordinates α and β may be selected as the Cartesian coordinates x and y with the following Lame′ parameters:

$$A = B = 1 \qquad 2\text{-}5$$

The shallowness parameter (λ) of an elliptical paraboloid shell forms, according to Stavridis, is as follows:

$$\lambda = \frac{f_1}{a} + \frac{1}{\gamma}\left(\frac{f_2}{b}\right) \qquad 2\text{-}6$$

2.6.1 Theory of Shallow Shells

Shallow shells are frequently used for roof structures of industrial and public buildings. It has also used in mechanical and aerospace engineering applications. The theory of shallow shells can be also used to analyze shells that become locally shallow when the original shell is divided into finite segments or elements [15].

If confine the analysis to the accuracy of the theory of thin shells, i.e., consider a shell as shallow for

$$\left(\frac{dz}{dx}\right)^2 < 0.05, \qquad \left(\frac{dz}{dy}\right)^2 < 0.05 \tag{2-7}$$

Then the angle of 0.224 rad or 13^0 may be taken as the limiting angle between the tangent plane to the shell's middle surface and the coordinate plane *Oxy*. Notice that Vlasov defined a shallow shell as a shell whose rise does not exceed 1/5 of the smallest dimension of the shell in its plane (projection on the coordinate plane *Oxy*).

Consider an element of the middle surface *ABCD* (figure-2.6 a). Let its projection on the coordinate plane *Oxy* be the rectangle with sides *dx* and *dy*, as shown in figure 2.6a. The sides of the element *ABCD* are the following:

$$ds_1 = \sqrt{1+\left(\frac{dz}{dx}\right)^2}dx \;; ds_2 = \sqrt{1+\left(\frac{dz}{dy}\right)^2}dy \tag{2-8}$$

However, under the assumption equation 2.8 it gives equation 2.4. i.e., one can identify the increments of arcs of the coordinate lines on the shell's middle surface with the increments of the corresponding rectangular coordinates. The cosine of the angle between the lines *x* and *y* is equal to

$$\cos\left(ds_1, ds_2\right) = \frac{\frac{dz}{dx}\frac{dz}{dy}}{\sqrt{\left(1+\left(\frac{dz}{dx}\right)^2\right)\left(1+\left(\frac{dz}{dy}\right)^2\right)}} \tag{2-9}$$

It follows from the above that for shallow shells, again because of the inequalities, one can assume that

$$\cos\left(ds_1, ds_2\right) \approx 0 \tag{2-10}$$

i.e., it is possible to consider the curvilinear system *x*; *y* as approximately orthogonal. The curvatures of the coordinate lines *x* and *y*, K_1 and K_2, and ''twist,'' K_{12}, of the undeformed

middle surface at any point of the middle surface of the shallow shell can be identified with the second derivatives of i.e.

$$k_1 = \frac{1}{R_1} \approx \frac{d^2 z}{dx^2}, k_2 = \frac{1}{R_2} \approx \frac{d^2 z}{dy^2}, k_{12} \approx \frac{d^2 z}{dxdy} \qquad 2\text{-}11$$

Taking equations 2.4 and 2.8 as exact equalities, it has obtained that the Lame´ parameters for a shallow shell of any geometry. i.e., the intrinsic geometry of a shallow shell is identical to the geometry of a plane of its projection. This represents the first basic assumption of the theory of shallow shells. It follows from the above that the shallow shell has the Gaussian curvature $\Gamma = \frac{1}{R_1 \times R_2} \approx 0$ because the latter is an exact zero only for flat plates. In particular cases, the Gaussian curvature of shallow shells is also exactly equal to zero (for instance, if a shallow shell is a cylindrical or conical shell).

The DMV (Donnell–Mushtari–Vlasov) theory [15] can be useful to the analysis of generally shallow shells form. Hence, the next, second basic assumption of the theory of shallow shells is the basic assumption of the more general DMV theory of neglecting the tangential (membrane) displacements *u* and *v* in the kinematic expressions for the changes in curvature and twist and the transverse shear forces Q_1 and Q_2 in the equations of equilibrium.

The DMV theory, as the general theory of thin shells, was constructed in terms of the lines of curvature as curvilinear coordinate lines. Therefore, from now on assume that the coordinate lines *x* and *y* coincide with the lines of curvature of the shell's middle surface.

The shallowness of shells makes it possible to make further simplifications to the DMV theory. Making $\alpha = x$; $\beta = y$; and $A = B = 1$, it has been obtained the following relations for the strain components and changes in curvature:

$$\varepsilon_1 = \frac{du}{dx} - \frac{w}{R_1}, \varepsilon_2 = \frac{du}{dy} - \frac{w}{R_2}, \gamma_{12} = \frac{du}{dx} + \frac{du}{dy}$$
$$\chi_1 = -\frac{d^2 w}{dx^2}, \chi_2 = -\frac{d^2 w}{dy^2}, \chi_{12} = -\frac{d^2 w}{dxdy} \qquad 2\text{-}12$$

The Laplace operator is easily simplified to the form

$$\nabla^2(...) = \frac{\partial^2(...)}{\partial x^2} + \frac{\partial^2(...)}{\partial y^2} \qquad 2\text{-}13$$

The Codazzi conditions for shallow shells, and taking into account equations are

$$\frac{\partial}{\partial \beta}\left(\frac{1}{R_1}\right) = 0 \;\; and \;\; \frac{\partial}{\partial \alpha}\left(\frac{1}{R_2}\right) = 0 \qquad 2\text{-}14$$

Also, the Vlasov operator $\nabla_k^{\,2}$, taking into account the above relations can be simplified to the following form:

$$\nabla_k(...) \equiv \frac{1}{R_1}\frac{\partial^2(...)}{\partial x^2} + \frac{1}{R_1}\frac{\partial^2(...)}{\partial y^2} = k_1\frac{\partial^2(...)}{\partial x^2} + k_2\frac{\partial^2(...)}{\partial x^2} \qquad 2\text{-}15$$

Thus, the system of the governing differential equations of the estimated DMV theory of thin shells have the following form:

$$\begin{aligned} &D\nabla^2\nabla^2\omega - \Phi\nabla_k^2 = P_3 \\ &\nabla^2\nabla^2\Phi - Eh\nabla_k^2 = 0 \end{aligned} \qquad 2\text{-}16$$

Having determined the above functions, it has then determined the internal forces and moments by shallow shell theory.

Let present below all these equations for shallow shells, as follows:

$$\begin{aligned} &N_1 = \frac{\partial^2\Phi}{\partial y^2}\,,\; N_2 = \frac{\partial^2\Phi}{\partial x^2}\,,\; N_{12} = \frac{\partial^2\Phi}{\partial x \partial y} \\ &M_1 = -D\left(\frac{\partial^2\omega}{\partial x^2} + \nu\frac{\partial^2\omega}{\partial y^2}\right),\; M_2 = -D\left(\frac{\partial^2\omega}{\partial y^2} + \nu\frac{\partial^2\omega}{\partial x^2}\right) \end{aligned} \qquad 2\text{-}17$$

2.7 Theoretical Analysis

The membrane theory for transitional shells of double curvatures is written by D. P Billington [16]. The following expressions are taken from that.

The equation for an elliptical paraboloid is

$$z = \frac{x^2}{h_1} + \frac{y^2}{h_2} \qquad 2\text{-}18$$

The constants h_1 and h_2 are

$$h_1 = \frac{a^2}{c_1} \text{ and } h_2 = \frac{b^2}{c_2} \qquad 2\text{-}19$$

Which clearly define the two sets of parabolas. If a horizontal plane is passed through the surface at $z_c = \text{constant}$, then

$$z_c = \frac{x^2}{h_1} + \frac{y^2}{h_2} = \text{constant}$$

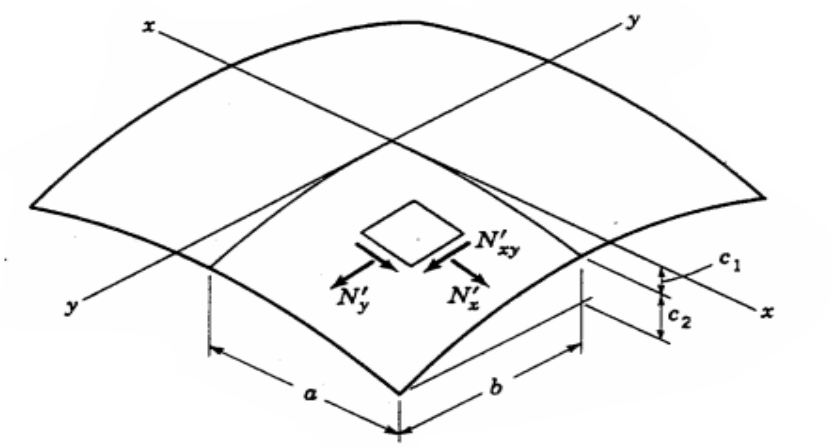

Figure 2-7: Geometry and stress resultant of elliptical paraboloid shell

Which defines an ellipse with semiaxis of

$$a_1 = \sqrt{z_c + h_1} \quad \text{and} \quad a_2 = \sqrt{z_c + h_2}$$

Hence the name elliptical paraboloid. In the special case where $h_1 = h_2$ then

$$z = \frac{x^2 + y^2}{h^2} \qquad 2\text{-}20$$

Which is a paraboloid of revolution since at $z_c = \text{constant}$,

$$z_c h_1 = x^2 + y^2$$

Thus planes normal to the *z*-axis intersect the surface in a circle of radius $r = \sqrt{z_c \times h_1}$

From the differential equation of equilibrium obtain

$$\frac{2}{h_2}\frac{\partial^2 F}{\partial x^2} + \frac{2}{h_1}\frac{\partial^2 F}{\partial y^2} = q \qquad 2\text{-}21$$

Take the simplifying assumption of loading uniformly distributed over the horizontal projection of the surface, $q = p_z$ .The problem is now to find a solution to the above equation which will at the same time satisfy reasonable boundary conditions. For example, if the boundaries $y = \pm b$ are to be supported by vertical arches which are not stiff laterally, a solution can be made by setting

$$F_0 = \frac{p_z h_1}{4}\left(b^2 - y^2\right) \qquad 2\text{-}22$$

$$N_x = \frac{\partial^2 F}{\partial y^2} - \int p_x dx = -\frac{p_z h_1}{2} = -\frac{p_z a^2}{2c_1}$$

$$N_y = \frac{\partial^2 F}{\partial x^2} - \int p_y dy = 0 \qquad 2\text{-}23$$

$$N_{xy} = -\frac{\partial^2 F}{\partial x \partial y} = 0$$

This assumption leads to an internal stress pattern in which all the load is carried by the arches parallel to the *x*-axis. There is no need for stiff arches along the edges $y = \pm b$, but stiff supports must be provided at $x = \pm a$ to carry the N_x forces or arch thrust, which can be written in the familiar form by recognizing that $N_x = H$ and $a = \frac{L}{2}$, so the first of the above equation can be written:

$$H = -\frac{PL^2}{8c_1}$$

Such a system is a form of barrel arch in which the arches do not spring from a straight line in the plan as a cylindrical barrel arch but from an elliptical curve.

To determine the internal stress distribution for such a case must choose F such that $N_x = 0$ at $x = \pm a$ and $N_y = 0$ at $y = \pm b$. Since the above equation satisfies only one or the other of these requirements, an additional force function is needed, which will be taken in the form of the infinite series:

$$F_1 = \sum_{n=1,3,5}^{\infty} A_n \cosh \beta x \cos \alpha y \qquad 2\text{-}24$$

where

$$\beta = \frac{n\pi}{2a}\sqrt{\frac{c_1}{c_2}}$$

and

$$\alpha = \frac{n\pi}{2b}$$

$$\frac{\partial^2 F}{\partial x^2} = \sum_{n=1,3,5}^{\infty} -A_n \beta^2 \cosh \beta x \cos \alpha y = N_y$$
$$\frac{\partial^2 F}{\partial y^2} = \sum_{n=1,3,5}^{\infty} A_n \alpha^2 \cosh \beta x \cos \alpha y = N_x \qquad 2\text{-}25$$

If F_1 combine with F_0, the result must give $N_y = 0$ at $y = \pm b$, which F_0 does alone and which F_0 give as $\left(\cos \frac{n\pi y}{2b} = 0 \quad \text{for } y = b\right)$, and it must also give $N_x = 0$ at $x = \pm a$

$$N_{x0} = -\frac{p_z a^2}{2c_1}$$

at $x = a$, and F_1 gives at $x = a$

$$N_{x1} = \sum_{n=1,3,5}^{\infty} -A_n \alpha^2 \cosh \beta x \cos \alpha y$$

$N_{x0} = N_{x1}$ must be zero $x = a$. First, it has expressed N_{x0} in terms of Fourier series

where

$$N_{x0} = -\left(\frac{p_z a^2}{2c_1}\right)\frac{4}{\pi}\sum_{n=1,3,5,\ldots}^{\infty}\frac{(-1)^{\left(\frac{n-1}{2}\right)}\cos\alpha y}{n}$$

To satisfy the boundary value of $N_x = 0$ at $x = \pm a$

$$\sum_{n=1,3,5}^{\infty} -A_n\alpha^2\cosh\beta x\cos\alpha y = -\left(\frac{p_z a^2}{2c_1}\right)\frac{4}{\pi}\sum_{n=1,3,5,\ldots}^{\infty}\frac{(-1)^{\left(\frac{n-1}{2}\right)}\cos\alpha y}{n}$$

The function $\cos\alpha y$ cancels out and

$$A_n = -\left(\frac{p_z a^2}{2c_1\pi}\right)\frac{1}{\alpha^2}\frac{(-1)^{\left(\frac{n-1}{2}\right)}}{\cos\beta a}$$

Substituting this value in the above equation

$$N_x = -\left(\frac{p_z a^2}{2c_1}\right)\left(\frac{2}{\pi}\sum_{n=1,3,5,\ldots}^{\infty}\frac{(-1)^{\left(\frac{n-1}{2}\right)}\cosh\beta x}{n\cosh\beta a}\cos\alpha y - \frac{1}{2}\right)$$

$$N_y = -\left(\frac{p_z b^2}{2c_1}\right)\left(\frac{2}{\pi}\sum_{n=1,3,5,\ldots}^{\infty}\frac{(-1)^{\left(\frac{n-1}{2}\right)}\cosh\beta x}{n\cosh\beta a}\cos\alpha y + 0\right) \qquad \text{2-26}$$

$$N_{xy} = -\left(\frac{p_z a\, b}{\sqrt{c_1 c_2}}\right)\left(\frac{2}{\pi}\sum_{n=1,3,5,\ldots}^{\infty}\frac{(-1)^{\left(\frac{n-1}{2}\right)}\sinh\beta x}{n\cosh\beta a}\sin\alpha y + 0\right)$$

Since the values within the parenthesis contain only the parameter $\frac{c_1}{c_2}$, they have been tabulated to simplify the computations.

$$N_x = -\left(\frac{p_z a^2 k}{c_1}\right)(\text{coefficient})$$
$$N_y = -\left(\frac{p_z b^2 k}{c_2}\right)(\text{coefficient})$$
$$N_{xy} = -\left(\frac{p_z a^2 k}{\sqrt{c_1 c_2}}\right)(\text{coefficient}) \qquad 2\text{-}27$$
$$k = \frac{\cos\theta}{\cos\phi} = \sqrt{\frac{1+\left[\left(\frac{2c_1}{a}\right)\left(\frac{x}{a}\right)\right]^2}{1+\left[\left(\frac{2c_2}{b}\right)\left(\frac{y}{b}\right)\right]^2}}$$

The coefficients are listed in tabular format in Appendix A. Finally it concludes that the internal force pattern satisfies the criteria that have no forces normal to the edges be allowed. From the elliptical paraboloid shape, all the load is carried along the free edges by tangential shear down to the corner supports, in the same manner as the hyperbolic paraboloid with straight-line generators as boundaries that is at the corners $x = \pm a$ and $y = \pm b$, the shear goes to infinity [16].

This may be taken as follow. In a translational surface, any element bounded by generators will have no twist in its surface. The tangential shearing forces on either side of the element are exactly parallel; hence the shear does not contribute to vertical equilibrium.

On the curves (edges) where $N_x = N_y = 0$ nothing is available to resist the vertical loads without the shearing forces. Thus transverse shearing forces and bending moments will occur to carry these loads, and the value N_{xy} will be determinate.

2.8 Stability Analysis

Generally to determine the stability of shells is the main concern for the design of the reinforced concrete shell structures now a day.

M. Farshad [13] explain the stability of any deformable bodies that may become unstable under certain loading conditions and thus have a premature failure. The phenomenon of instability is particularly important for thin shells subjected to compressive forces. In such cases, the loadings which produce instability modes of failure are several orders of

magnitudes smaller than the forces causing the material collapse of the structure. A special mode of shell instability is the buckling of shells which occurs under certain static or dynamic loading conditions.

The design of thin shells is normally dominated by the stability considerations and not merely the material strength requirements. Hence, the stability analysis of thin shells acquires prime importance in various problems related to the design of shells.

2.9 Concepts of Stability and Instability

M. Farshad [13] also stated the idea behind the reality of stability and instability of any deformable bodies. Instability is a universal phenomenon that may occur in various material bodies. The fundamental concepts of stability and instability are clarified through the following definitions:

The state of a system is the collection of values of the system parameters at any instant of time. For example, the positions of material points in a structure and the temperature field at various points constitute the state of that system. The state of a system depends on system parameters and environmental conditions. For example, in a shell structure, the system parameters are geometrical and material properties, and the environmental conditions are the applied forces and thermal conditions.

2.10 Stability

The state of a system, at any instant of time, is called stable if the relatively small changes in system parameters and/or environmental conditions would bring about relatively small changes in the existing state of the system.

2.11 Instability

The state of a system at any instant of time is called unstable if relatively small changes in system parameters and/or environmental conditions would cause major changes in the existing state.

Buckling is a special mode of the instability of equilibrium which may occur in deformable bodies subjected mostly to compressive loadings [13].

2.12 Buckling of Elliptic Paraboloid Shell

Elliptic paraboloid shell is a doubly curved, synclastic, and non-developable surface. Therefore, it is generally very strong and highly stable. The critical stability load of the elliptic paraboloid shell is usually much higher than those of concrete shells with single curvature. Nevertheless, thin concrete elliptic paraboloid with a large span is susceptible to buckling; indeed the buckling consideration is one of the main design criteria of such shell [13].

The theoretical buckling load for a doubly curved elastic shell having the values of principal curvature $\frac{1}{R_1}$ and $\frac{1}{R_2}$, under the dead load, is

$$p_{cr} = \frac{2Et^2}{\sqrt{3\left(1-\nu^2\right)}} \frac{1}{R_1} \frac{1}{R_2} \qquad 2\text{-}28$$

and used in this research paper for the determination of critical pressure p_{cr} for an elliptical paraboloid shell.

2.13 For Design of Elliptic Parabolic Shell

To prevent buckling of a convex reinforced concrete shell, the design load F_d that acts on the shell, should not exceed the critical buckling load p_{cr}, i.e.

$$F_d = p_{cr} \qquad 2\text{-}29$$

where p_{cr} is calculated using the following expression that is presented in a book design principle and analysis of thin concrete shells, domes, and folder by I. Iskhakov and Y. Ribakov [17].

$$p_{cr} = 0.2 E_{crd} \left(\frac{h}{R_{\max}} \right)^2 \times k \qquad 2\text{-}30$$

E_{crd} is the reduced modulus of elasticity of concrete that considers concrete creep that decreases the load-carrying capacity of statically undetermined structures with time. When the surrounding environment humidity is higher than 40%

$$E_{crd} = 0.319 E_c \qquad 2\text{-}31$$

else

$$E_{crd} = 0.212 E_c \qquad 2\text{-}32$$

where h is the shell's thickness; $R_{\max}$ is the maximum value of the radius of curvature for translation shell (the radius of curvature in the other direction is the minimum one $R_{\min}$); k is a coefficient that depends on the ratio $R_{\max}/R_{\min}$ following

Table 2-2: Coefficients k vs. R_{max} / R_{min} ratio

$R_{\max}/R_{\min}$	< 1.5	1.5	1.75	2	2.25	2.5	> 2.5
k	1	1.17	1.4	1.63	1.79	1.98	2

2.14 Free Vibration

The free vibration of the general shallow shell is described below obtained from the book thin plates and shells [15].

Assume that the state of stress within a shell during vibrations has a character determined by the equations of equilibrium, and the shell middle surface deforms according to the same law during vibrations as in the static equilibrium state. The equations of motion of the vibrating shell can be obtained by applying the D'Alambert principle, – i.e., by adding the inertia forces to given external loads, assigned by components P_1; P_2; and P_3, namely (damping forces are not considered here):

$$p_1 \to p_1 - \rho h \frac{\partial^2 u}{\partial t^2},\ p_2 \to p_2 - \rho h \frac{\partial^2 v}{\partial t^2}, p_3 \to p_3 - \rho h \frac{\partial^2 w}{\partial t^2} \qquad 2\text{-}33$$

where P_1, P_2, P_3, and u, v, w, are functions of the Cartesian coordinates of the middle surface and time, ρ is the mass density of the material, and h is the shell thickness. Free vibrations of shells occur in the absence of applied loads but are initiated by some initial conditions imposed on the shell, and forced vibrations of shells, which result from the application of time-dependent loads.

The governing differential equations of free vibrations of shallow shells can be obtained by setting $P_1 = P_2 = P_3 = 0$ and assuming that stiffness of the shell in the middle surface is much greater than its stiffness in the direction normal to the middle surface. Therefore, putting $\alpha = x$ and $\beta = y$ and neglecting the in-plane inertia forces, it obtains the following differential equations of free vibrations of shallow shells:

$$\begin{aligned} D\nabla^2\nabla^2 w - \nabla_k^2 \Phi + \rho h \frac{\partial^2 w}{\partial t^2} = 0 \\ \nabla^2\nabla^2 \Phi - Eh\nabla_k^2 w = 0 \end{aligned} \qquad 2\text{-}34$$

The natural frequency of free vibrations of a shallow shell for the simply supported shell of double curvature.

$$\omega_{mn}^2 = \frac{1}{\rho h}\left[D\left(\lambda_{mn}^2 + \mu_{mn}^2\right)^2 + \frac{Eh\left(\frac{\lambda_n^2}{R_1} + \frac{\mu_m^2}{R_2}\right)^2}{\left(\lambda_n^2 + \mu_m^2\right)^2} \right] \qquad 2\text{-}35$$

where

$$\lambda_n = \frac{n\pi}{a};$$

$$\mu_m = \frac{m\pi}{b};$$

$$D = \frac{Eh^3}{12(1-\nu^2)}$$

Equations of a minimum $\frac{\partial \omega_{mn}^2}{\partial \lambda_n} = 0$ for a fixed value of μ_m and $\frac{\partial \omega_{mn}^2}{\partial \mu_{mn}} = 0$ for a fixed value of λ_n have no real roots, which shows the monotonic character of the variation of ω_{mn}^2 as a function of λ_n and μ_m. Thus, the frequency of the fundamental mode, or the lowest natural frequency of free vibrations of a given shallow, simply supported shell, corresponds to one half-wave in the x and y-directions, i.e. $m = n = 1$.

As stated by the book of W. Sodel [18] in the vibration of plates and shell. Simply supported doubly curved shell is analyzed by

$$\omega_{mnc}^2 = \omega_{mnf}^2 + \frac{\left[\frac{1}{R_y}\left(\frac{m\pi}{a}\right)^2 + \frac{1}{R_x}\left(\frac{n\pi}{b}\right)^2\right]^2}{\left[\left(\frac{m\pi}{a}\right)^2 + \left(\frac{n\pi}{b}\right)^2\right]}\left(\frac{E}{\rho}\right) \qquad 2\text{-}36$$

where

ω_{mnf}^2 is the equivalent frequency for the flat plate

$$\omega_{mnf} = \pi^2\left[\left(\frac{m}{a}\right)^2 + \left(\frac{n}{b}\right)^2\right]\sqrt{\frac{D}{\rho h}} \qquad 2\text{-}37$$

CHAPTER 3 MATERIAL AND ANALYSIS METHODS

3.1 Material

For this study C20/25, C40/50, and C60/75 concrete types [19] are taken for the determination of critical buckling load. For the analysis of internal forces and free vibration structural concrete C20/25 with a young's modulus of 30 GPa, Poisson's ratio of 0.2 and a unit weight of 25 kN/m^3 were used. The partial safety factors for all the reinforced concrete resistance were taken as γ_m=1. The brief material property is listed in the sample solved model. The finite element software RFEM is used for modeling and analysis of thin elliptic paraboloid shell. For theoretical analysis of a thin shell MATLAB R2019b [20] is essential in this research.

3.2 Geometry

The geometrical property and the procedures followed in the theoretical and numerical analysis of each modeled shell is described in a sample solved problem. T. Nagy [4] considered geometric details of the elliptic curve generator, which is a positive Gaussian curvature, as shown in figure 3-1.

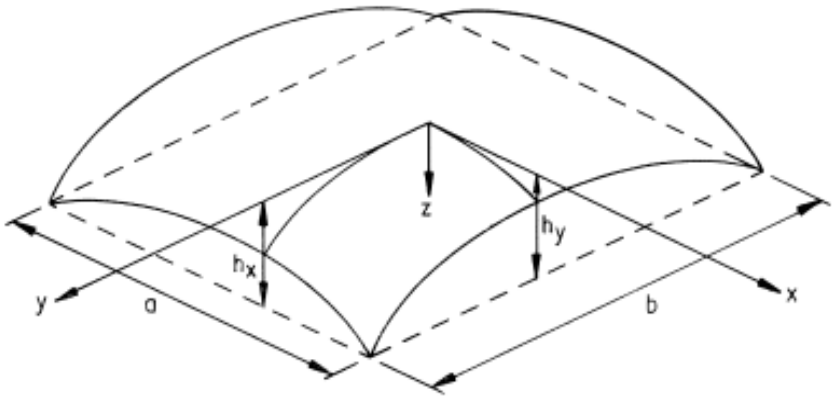

Figure 3-1: Elliptic paraboloid shell geometry

The general equation for elliptic paraboloid shell according to T. Nagay

$$z = -4h_x\left(\frac{x}{a} - \frac{x^2}{(a)^2}\right) - 4h_y\left(\frac{y}{b} - \frac{y^2}{(b)^2}\right) \quad 3\text{-}1$$

where

h_x = is the rise of the shell in the *x*-direction

h_y = is the rise of the shell in the *y*-direction

x and a dimension in the *x*-direction

y and b dimension in the *y*-direction

3.3 Parametric Study

The impact of thickness, the radius of curvature, rise of curvature in *x* and *y*-direction, and the dimension of elliptic parabolic in terms of the square and rectangular plan in critical buckling of the load. And also the influence of thickness on natural vibration of the shell by its weight. For the analysis of buckling load and natural vibration simply supported boundary condition is considered.

Table 3-1: Geometrical parameter for models

Description	**Symbols**	**Values(m)**
The thickness of the shell	*h*	0.050 - 0.150
Rise of the shell in the *x*-direction	f_1 *or* h_x	0.500 - 0.800
Rise of the shell in the *y*-direction	f_2 *or* h_y	0.500
The dimension of the shell in the *x*-direction	*a*	5.000
The dimension of the shell in the *y*-direction	*b*	4.000 and 5.000
The radius of curvature in rectangular plan Elliptic paraboloid shell *x*-direction	R_1 *or* R_x	15.625 and 17.857
The radius of curvature in rectangular plan Elliptic paraboloid shell *y*-direction	R_2 *or* R_y	16.000
The radius of curvature in square plan elliptic Paraboloid shell *x*-direction	R_1 or R_x	15.625 - 25.000
The radius of curvature in square plan elliptic Paraboloid shell *y*-direction	R_2 or R_y	15.625 - 25.000

3.4 Calculation of Internal Forces by Theoretical Method

Material Properties;

- Young's modulus (E) = 30000 MPa
- Poisons ratio (μ) = 0.2
- The mass densities of the shell (ρ) = 2500 kg/m^3

Geometric Properties;

- Dimension: $2a$ = 10m and $2b$ = 8m
- Radius of curvature: R_1= 25m and R_2 = 20m
- Thickness of the elliptic parabolic shell : t = 0.1m
- Raise of the shell: $f_1 = C_1$ = 0.5m and $f_2 = C_2$ = 0.5m

Self weight (Dead Load) = Unit weight of concrete × Thickness of the shell

$$P = 25.000 \text{ kN/m}^3 \times 0.100\text{m}$$

$$P = 2.500 \text{ kN/m}^2$$

It has used three theoretical methods to calculate the internal force of the elliptic paraboloid shell.

3.4.1 Analyzed by Table of Coefficient

- Ny result in the central y-direction

$$N_y = -\frac{p \times b^2}{C_2} \times k \times F3 = -31.250 kN/m \quad \text{at} \quad x = 0.000m \,\text{and} \quad y = 0.000m$$

- Nx result in the central x-direction

$$k=\sqrt{\frac{1+\left[\left(\frac{2c_1}{a}\right)\left(\frac{x}{a}\right)\right]^2}{1+\left[\left(\frac{2c_2}{b}\right)\left(\frac{y}{b}\right)\right]^2}}=\sqrt{\frac{1+\left[\left(\frac{2.000\times0.500m}{5.000m}\right)\left(\frac{0.000}{5.000m}\right)\right]^2}{1+\left[\left(\frac{2.000\times0.500m}{4.000m}\right)\left(\frac{0.000}{4.000m}\right)\right]^2}}=1.000$$

at $x=0.000m$ and $y=0.000m$

$$N_x=-\frac{p\times a^2}{C_1}\times k\times F1=-31.250\,kN/m$$

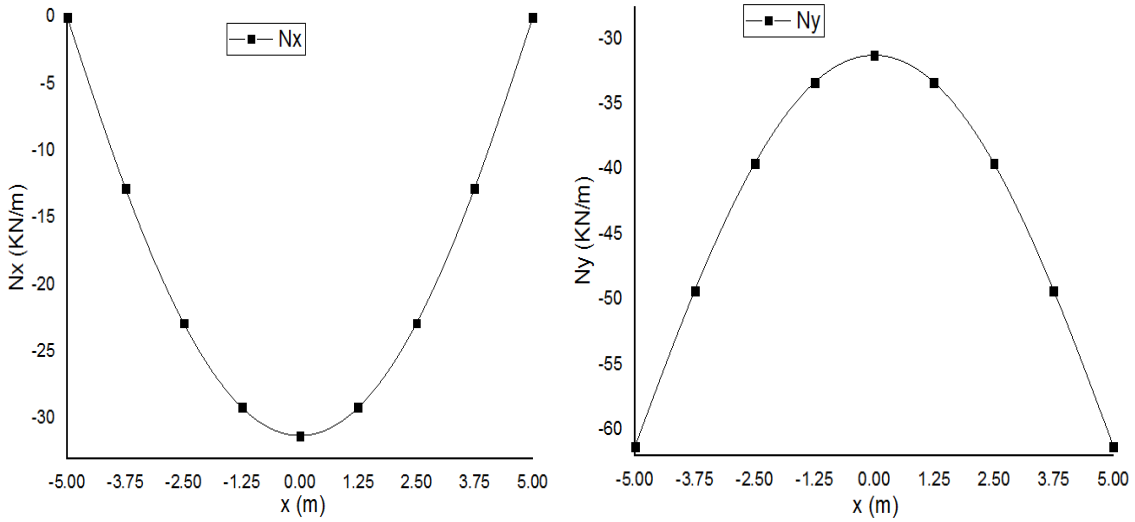

Figure 3-2: Internal force diagram in the central section of the *x*-direction

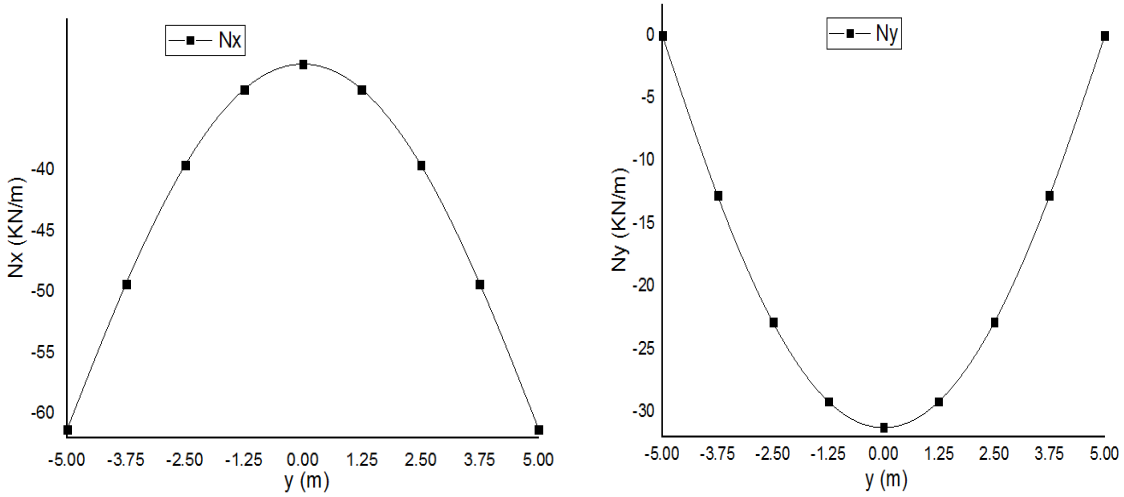

Figure 3-3: Internal force diagram in the central section of the *x*-direction

- *Nxy* result in the central *x* and *y*-direction

$$N_{xy} = -\frac{p \times a \times b}{\sqrt{C_1 \times C_2}} \times F3 = 0.000 kN/m$$

- *Nxy* is zero in the central section of the shell in the *x* and *y*-direction

N.B:- *F1*,*F2* & *F3* value is read from the table in appendix A.

3.4.2 Analyzed by Shallow Shell Theory (DMV Theory)

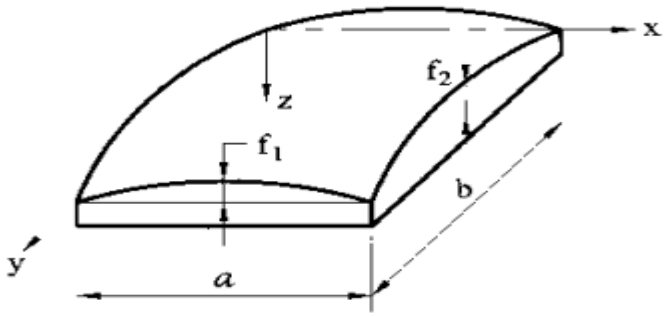

Figure 3-4: Elliptic parabolic shell

$$z = f_1 \frac{x^2}{a^2} + f_2 \frac{y^2}{b^2} \qquad 3\text{-}2$$

Step 1. Determine the principal curvatures of the shell by equation 2.11.

$$k_1 = \frac{\partial^2 z}{\partial x^2} = \frac{2f_1}{a^2},\ k_1 = \frac{\partial^2 z}{\partial y^2} = \frac{2f_2}{b^2},\ k_{12} \approx \frac{\partial^2 z}{\partial x \partial y} = 0$$

Step 2. Substituting the above into the expressions in equation 2.16.

The system of equations above in the above, as follows (making $P_3 = P_0$):

$$\begin{aligned} D\nabla^2\nabla^2\omega - \frac{2h_1}{b^2}\frac{\partial^2\Phi}{\partial x^2} &= p_0 \\ \frac{1}{Et}\nabla^2\nabla^2\Phi + \frac{2h_2}{b^2}\frac{\partial^2\omega}{\partial x^2} &= 0 \end{aligned} \qquad 3\text{-}3$$

Step 3. The boundary conditions on the shell edges.

$$\begin{aligned}
&\omega = 0 \,|\, x = 0, a; \;\; \frac{\partial^2 \omega}{\partial x^2} = 0 \,|\, x = 0, a; \\
&\frac{\partial^2 \Phi}{\partial y^2} = 0 \,|\, x = 0, a; \;\; \nu = 0 \,|\, x = 0, a; \\
&\omega = 0 \,|\, y = 0, b; \;\; \frac{\partial^2 \omega}{\partial y^2} = 0 \,|\, y = 0, b; \\
&\frac{\partial^2 \Phi}{\partial x^2} = 0 \,|\, y = 0, b; \;\; u = 0 \,|\, y = 0, b;
\end{aligned} \qquad 3\text{-}4$$

Step 4. A solution of step 2 is sought in the following form of the Fourier series in two variables:

$$\begin{aligned}
\omega &= \sum_{n=1}^{\infty} \sum_{m=1}^{\infty} \omega_{mn} \sin \frac{m\pi x}{a} \sin \frac{n\pi y}{b} \\
\Phi &= \sum_{n=1}^{\infty} \sum_{m=1}^{\infty} \Phi_{mn} \sin \frac{m\pi x}{a} \sin \frac{n\pi y}{b}
\end{aligned} \qquad 3\text{-}5$$

Step 5. It can be shown that the expressions of ϕ and ω satisfy exactly the three first conditions in step 3. Let it check the fulfillment of the fourth condition. Find the strain, as follows:

$$\varepsilon_2 = \frac{1}{Et}\left(N_2 - \nu N_1\right) = \frac{1}{Et}\left(\frac{\partial^2 \Phi}{\partial x^2} - \nu \frac{\partial^2 \Phi}{\partial y^2}\right) \qquad 3\text{-}6$$

Substituting for φ from step 4 into the above equation results in the following:

$$\varepsilon_2 = \frac{1}{Et} \sum_{n=1}^{\infty} \sum_{m=1}^{\infty} \Phi_{mn} \left(\frac{m^2\pi^2}{a^2} - \nu \frac{n^2\pi^2}{b^2}\right) \sin \frac{m\pi x}{a} \sin \frac{n\pi y}{b} \qquad 3\text{-}7$$

It is evident, that $\varepsilon_2 = 0 \; for \; x = 0 \; and \; x = a.$

Similarly, it is possible to show that the displacement $u = 0$ along edges $y = -b$ and $y = b$:

Step 6. Next, represent the given load P_0 in the form of the Fourier series too, as follows:

$$p_{mn} = \sum_{n=1}^{\infty} \sum_{m=1}^{\infty} p(x,y) \sin\frac{m\pi x}{a} \sin\frac{n\pi y}{b} \qquad 3\text{-}8$$

$$p(x,y) = \sum_{n=1}^{\infty} \sum_{m=1}^{\infty} p_{mn} \sin\frac{m\pi x}{a} \sin\frac{n\pi y}{b} \qquad 3\text{-}9$$

where

$$p_{mn} = \frac{4}{ab} \int_0^a \int_0^b p(x,y) \sin\frac{m\pi x}{a} \sin\frac{n\pi y}{b} dxdy \qquad 3\text{-}10$$

since

$$p(x,y) = p_0 = \text{constant, then } p_{mn} = \frac{16 p_0}{mn\pi^2};\ m,n = 1,3,5,...$$

Inserting the expressions of step 4, and 6 into step 2, it obtained the following system of linear algebraic equations:

$$\frac{1}{Et}\Phi_{mn}\left(\frac{m^2\pi^2}{a^2}+\frac{n^2\pi^2}{b^2}\right)^2 - \frac{2\pi^2\omega_{mn}}{a^2b^2}\left(m^2h_2+n^2h_1\right) = 0$$

$$D\omega_{mn}\left(\frac{m^2\pi^2}{a^2}+\frac{n^2\pi^2}{b^2}\right)^2 + \frac{2\pi^2\Phi_{mn}}{a^2b^2}\left(m^2h_2+n^2h_1\right) = p_{mn}$$

Solving this system for unknown functions ω_{mn} and ϕ_{mn}, gives

$$\Phi_{mn} = \frac{2b^2Et}{n^2\pi^2a^2A_{mn}}\left(f_1+\frac{m^2f_2}{n^2}\right)\omega_{mn}$$

$$\omega_{mn} = \left[\frac{t^4\pi^4n^4A_{mn}}{12\left(1-\nu^2\right)b^4} + \frac{4t^2\left(f_1+\frac{m^2}{n^2}f_2\right)^2}{a^4A_{mn}}\right]^{-1}\frac{tp_{mn}}{E} \qquad 3\text{-}11$$

where

$$A_{mn} = \left(1+\frac{m^2b^2}{n^2a^2}\right)^2;\ m,n = 1,3,5,...$$

$$\Phi_{mn} = \frac{8b^2 E t n^4 \times 0.5\left(\frac{m^2+n^2}{n^2}\right)}{n^2\pi^2 a^2\left(m^2+n^2\right)} = \frac{4Et\omega_{mn}}{\pi^2(m^2+n^2)}, \qquad \text{at } a=b$$

$$\omega_{mn} = \left[\frac{t^4\pi^4 n^4 A_{mn}}{12\left(1-\nu^2\right)b^4} + \frac{4t^2\left(f_1+\frac{m^2}{n^2}f_2\right)^2}{a^4}\right]^{-1} \frac{16t\times p_0}{E\pi^2 mn}, \qquad \text{at } a=b$$

Having determined the functions w and φ, the internal forces and moments may be found

$$\begin{aligned}
N_1 &= \frac{\partial^2\Phi}{\partial y^2} = -\sum_{m=1}^{\infty}\sum_{n=1}^{\infty}\Phi_{mn}\frac{n^2\pi^2}{b^2}\sin\frac{m\pi x}{a}\sin\frac{n\pi y}{b}\\
N_2 &= \frac{\partial^2\Phi}{\partial x^2} = -\sum_{m=1}^{\infty}\sum_{n=1}^{\infty}\Phi_{mn}\frac{m^2\pi^2}{a^2}\sin\frac{m\pi x}{a}\sin\frac{n\pi y}{b}\\
N_{12} &= -D\sum_{m=1}^{\infty}\sum_{n=1}^{\infty}\Phi_{mn}\frac{mn\pi^2}{ab}\cos\frac{m\pi x}{a}\cos\frac{n\pi y}{b}\\
M_1 &= D\sum_{m=1}^{\infty}\sum_{n=1}^{\infty}\omega_{mn}\left(\frac{\nu n^2\pi^2}{b^2}+\frac{m^2\pi^2}{a^2}\right)\sin\frac{m\pi x}{a}\sin\frac{n\pi y}{b}\\
M_2 &= D\sum_{m=1}^{\infty}\sum_{n=1}^{\infty}\omega_{mn}\left(\frac{n^2\pi^2}{b^2}+\frac{\nu m^2\pi^2}{a^2}\right)\sin\frac{m\pi x}{a}\sin\frac{n\pi y}{b}\\
M_{12} &= -D(1-\nu)\sum_{m=1}^{\infty}\sum_{n=1}^{\infty}\omega_{mn}\frac{nm\pi^2}{ab}\cos\frac{m\pi x}{a}\cos\frac{n\pi y}{b}
\end{aligned} \qquad \text{3-12}$$

Some numerical values of the deflections, internal forces, and moments were calculated with the use of equation 3-12 for the given shallow shell. The values of dimensionless coefficients w; M; N is given in the table in an appendix at the central point of the square shallow shell ($a = b$) for various dimensionless parameters $\lambda = \frac{f}{h}$ (λ characterizes the shallowness of a shell and $f = C_1 + C_2 = f_1 + f_2$). The values of the deflections, internal forces, and moments are determined from the following relations.

$$\omega = \bar{\omega} \times \frac{p_0 \times a^4}{D \times 10^4};\ N_1 = N_2 = \bar{N} \times \frac{p_0 \times a^4}{h \times 10^2};\ M_1 = M_2 = \bar{M} \times \frac{p_0 \times a^2}{10^2} \qquad 3\text{-}13$$

$$\lambda = \frac{f_1 + f_2}{h} = \frac{1.0m}{0.1m} = 10.000$$

$$N_1 = N_2 = \bar{N} \times \frac{p_0 \times a^4}{h \times 10^2} = -1.310 \times \frac{2.5 \times 10^4}{0.1 \times 10^2} = -32.755\,kN/m$$

$$M_1 = M_2 = \bar{M} \times \frac{p_0 \times a^2}{10^2} = -0.022 \times \frac{2.500 \times 10^2}{10^2} = -0.055\,kN.m/m$$

$$D = \frac{Eh^3}{12\left(1-\nu^2\right)} = \frac{30 \times 10^6 \times 0.1^3}{12\left(1-0.2^2\right)} = 2.604MN.m$$

$$\omega = \bar{\omega} \times \frac{p_0 \times a^4}{D \times 10^4} = 0.560 \times \frac{2.5 \times 10^7}{2.604 \times 10^{10}} = 537.689 \times 10^{-6} m = 0.538mm$$

- Internal forces and moments diagrams in the central *x*-direction

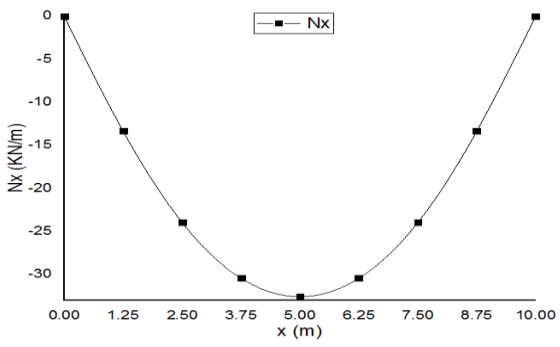

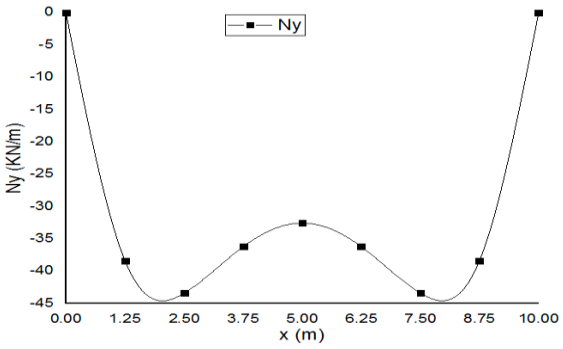

:

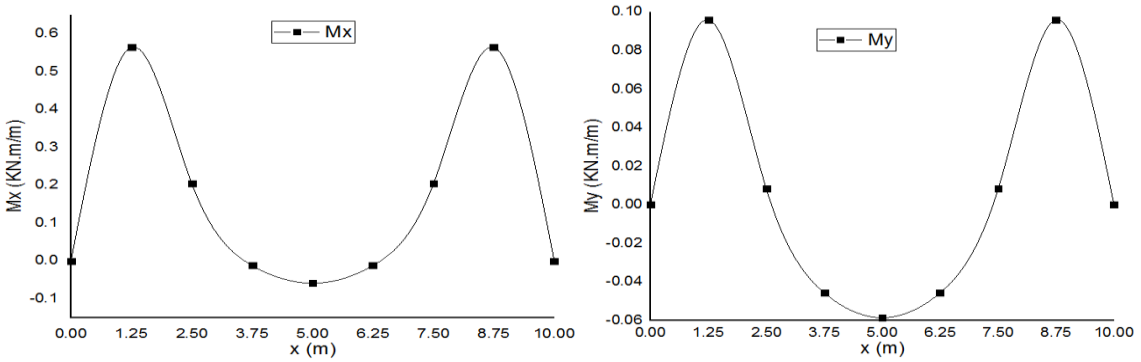

Figure 3-5: Internal forces and moments in the *x*-direction

- Internal forces and moments diagrams in the central *y*-direction

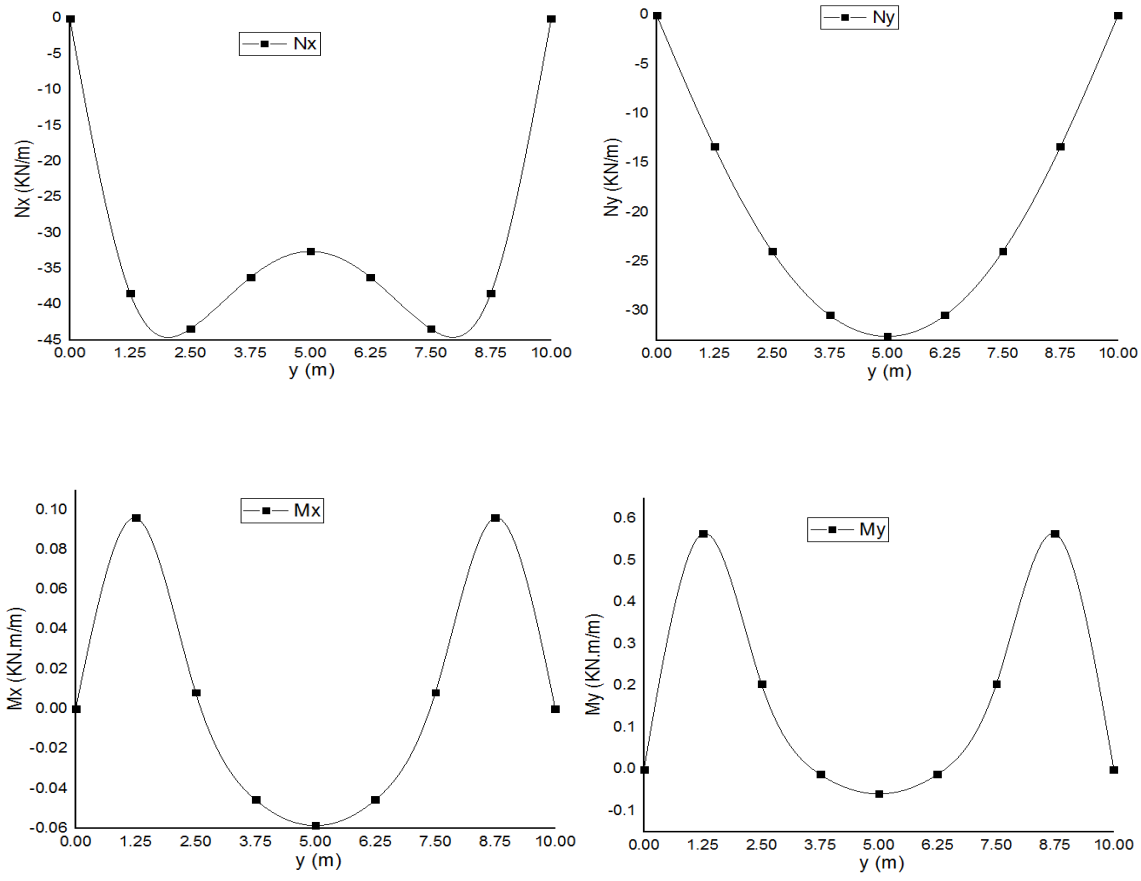

Figure 3-6: Internal forces and moments in the *y*-direction

N.B Internal force *Nxy* and moment *Mxy* is zero in the central *x* and *y*-direction

- Internal forces and moments diagrams around the boundary in the *x*-direction

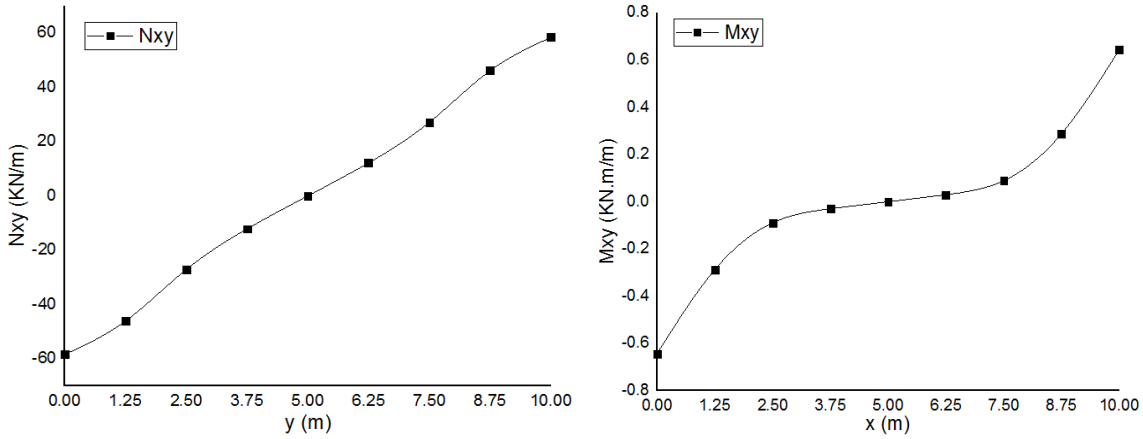

Figure 3-7: Internal force and moment around the boundary

- Deformation diagram in the central *x* and *y*-direction

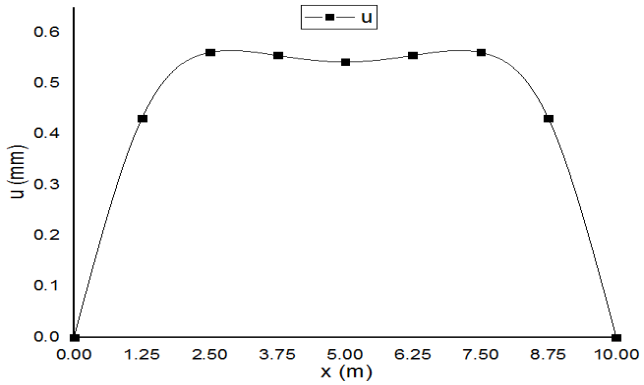

Figure 3-8: Deformation in the central section

3.4.3 Analyzed by Exponential Algebraic Polynomial

The internal force of the convex transition square and the rectangular shell is calculated and determined by the exponential algebraic polynomial formulas that are suggested by the I. Iskhakov and Y.Ribakov [17]. They supposed that the stresses' function at the edges for symmetric external loading and system of coordinate should be an even function, i.e., it should be signified by an exponential algebraic polynomial. Therefore, just elements with even exponents should remain. The function should be selected so that its first term $\varphi 1\ (x, y)$ satisfies the solution of the equation below

$$k_x N_x + k_y N_y + 2k_{xy} N_{xy} = -p \qquad 3\text{-}14$$

in the first estimate, and the other terms $\varphi 2\,(x, y)$, $\varphi 3\,(x, y)$, …, $\varphi i\,(x, y)$ improve the solution accuracy. For realizing these requirements for $i = 3$, it is possible to assume the stresses' function in the following form:

$$\varphi_i(x, y) = \varphi_i(x)\varphi_i(y) = a_1 A_{x1} A_{y1} + a_2 A_{x2} A_{y1} + a_3 A_{x1} A_{y2} \qquad 3\text{-}15$$

where

$$A_{x1} = x^4 - 6x^2 a^2 + 5a^4$$
$$A_{y1} = y^4 - 6y^2 b^2 + 5b^4$$
$$A_{x2} = x^8 - 2.444x^4 a^2 + 1.444x^4 a^4$$
$$A_{y2} = y^8 - 2.444y^4 b^2 + 1.444y^4 b^4$$

The internal membrane forces can be calculated

$$N_x = 12a_1 A_{x1}(y^2 - b^2) + 12a_2 A_{x2}(y^2 - b^2) + 4a_3 A_{x1} B_y \qquad 3\text{-}16$$

where

$$B_y = 14y^6 - 18.333y^4 b^2 + 4.333y^2 b^4$$

$$N_y = 12a_1 A_{y1}(x^2 - a^2) + 12a_2 A_{y2}(x^2 - a^2) + 4a_3 A_{y1} B_x \qquad 3\text{-}17$$

and

$$B_x = 14x^6 - 18.333x^4 a^2 + 4.333x^2 a^4$$

$$-N_{xy} = 16(a_1 C_x C_y + a_2 D_x C_y + a_3 C_x D_y) \qquad 3\text{-}18$$

where

$$C_x = x^3 - 3xa^2$$
$$C_y = y^3 - 3yb^2$$
$$D_x = 2x^7 - 3.666x^5 a^2 + 1.444x^3 a^4$$
$$D_y = 2y^7 - 3.666y^5 b^2 + 1.444y^3 b^4$$

Parameters a_i ($i = 3$) can be calculated, using the following expressions:

$$a_1 = \frac{qR_1}{60a^4\lambda(\lambda+\mu_k)}$$
$$a_2 = \frac{qR_2 - a_1a^6\lambda(11.4\lambda+9.552\mu_k)}{a^{10}\lambda(21.655\lambda+0.972\mu_k)} \qquad 3\text{-}19$$
$$a_3 = \frac{qR_2 - a_1a^6\lambda(11.4\lambda+9.552\mu_k)}{a^{10}\lambda^3(21.655\lambda+0.972\mu_k)}$$

where

$$\lambda = \left(\frac{b}{a}\right)^2 \;;\; 0.5a \le b \le a \;;\; \mu_k = \frac{K_1}{K_2} = \frac{R_2}{R_1} \qquad 3\text{-}20$$

In the above expressions, *a* and *b* are half of the rectangular shell spans in *x* and *y*-directions, respectively.

In order to select parameters a_i (i = 1, 2, 3), three co-location points are used. The coordinates of these points are:

$$A(0,0),\quad B(0,9b),\quad C(0.9a,0) \qquad 3\text{-}21$$

The selection of these points is not random but depends on the distribution of the normal membrane forces' *Nx* and *Ny* in the shell, which is known from the shell theory and experimental investigations.

For the above geometrical property of elliptical paraboloid shell at the center (x = 0 and y = 0)

$$\lambda = \left(\frac{b}{a}\right)^2 = \left(\frac{5m}{5m}\right)^2 = 1,\;\; \mu_k = \frac{R_2}{R_1} = \frac{25m}{25m} = 1$$

$$A_{x1} = x^4 - 6x^2a^2 + 5a^4 = 5a^4$$
$$A_{y1} = y^4 - 6y^2b^2 + 5b^4 = 5b^4$$
$$A_{x2} = A_{y2} = B_x = B_y = 0$$

Therefore the only required values of parameters a_i (i = 3) is a_1

$$a_1 = \frac{qR_1}{60a^4\lambda(\lambda+\mu_k)} = \frac{qR_1}{120a^6}$$

$$N_x = 12a_1A_{x1}(y^2-b^2)+12a_2A_{x2}(y^2-b^2)+4a_3A_{x1}B_y$$
$$= 12a_1A_{x1}(-b^2) = 12\frac{qR_1}{120a^6}\times 5a^4\times(-5^2) = -31.250kN/m$$
$$N_y = 12a_1A_{y1}(x^2-a^2)+12a_2A_{y2}(x^2-a^2)+4a_3A_{y1}B_x$$
$$= 12a_1A_{y1}(-a^2) = 12\frac{qR_1}{120a^6}\times 5b^4\times(-5^2) = -31.250kN/m$$

Table 3-2: Result of internal forces

x	*y*	*Nx* (kN/m)	*Ny* (kN/m)	*Nxy* (kN/m)
-5.000	-5.000	0.000	0.000	0.000
-4.500	-4.500	-54.375	-54.375	0.000
0.000	0.000	-31.250	-31.250	0.000
4.500	4.500	-54.375	-54.375	0.000
5.000	5.000	0.000	0.000	0.000

3.5 Finite Element Analysis

3.5.1 General Information

In this study, it has used finite element analysis software to determine internal forces in the elliptic paraboloid shell structure, and to obtain the critical buckling load of the shell under its weight in a similar way it helps to find the free vibration.

3.6 RFEM Analysis

3.6.1 Introduction to RFEM

RFEM is spatial models calculated according to the finite element method. It is invented by the DLUBAL SOFTWARE GmbH company. It is established in 1987, develops powerful and user-friendly engineering software for structural and dynamic analysis and design. Since 1990, the company's headquarters is located in Tiefenbach in eastern Bavaria, Germany [21].

The structural FEA software RFEM for analysis and design of plates, walls, shells, solids, and frame structures is a powerful program performing various tasks of modern civil engineering. The program is the basis of a modular software system: RFEM determines

internal forces, deformations, and support reactions of general plate structures with or without member and solid elements.

3.6.2 Finite Element Modeling

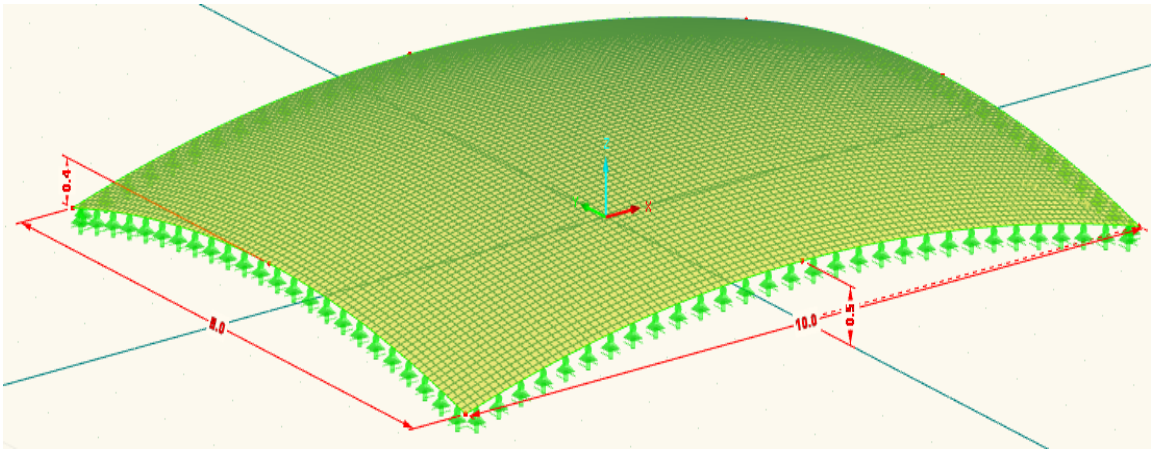

Figure 3-9: Elliptic paraboloid shell model

For the use of numerical analysis in this research it has been used RFEM 5.31

3.6.3 Analysis Procedures for Internal Forces and Moments

Basic internal force result of elliptic parabolic shell structure by RFEM.

Procedures

Step 1. Create nodes at the required distance.

Step 2. Connect three nodes in the *x*, *y,* and *z*-direction by a parabola.

Step 3. Make a quadrangle (General four-sided surface) by selecting parabolic arches.

Step 4. Define material

Step 5. If required add load case and load combination.

Step 6. Add support around the shell surface. (Diagphram support, meaning that translational degree of freedom parallel to the plane containing the curve is prohibited.)

Step 7. Generate finite element mesh

Step 8. Analysis(calculate) all the required results.

- Internal Forces Results

Nx in the central *x*-direction $N_x = -32.519\,kN/m$ at $x = 0.000m$ and $y = 0.000m$

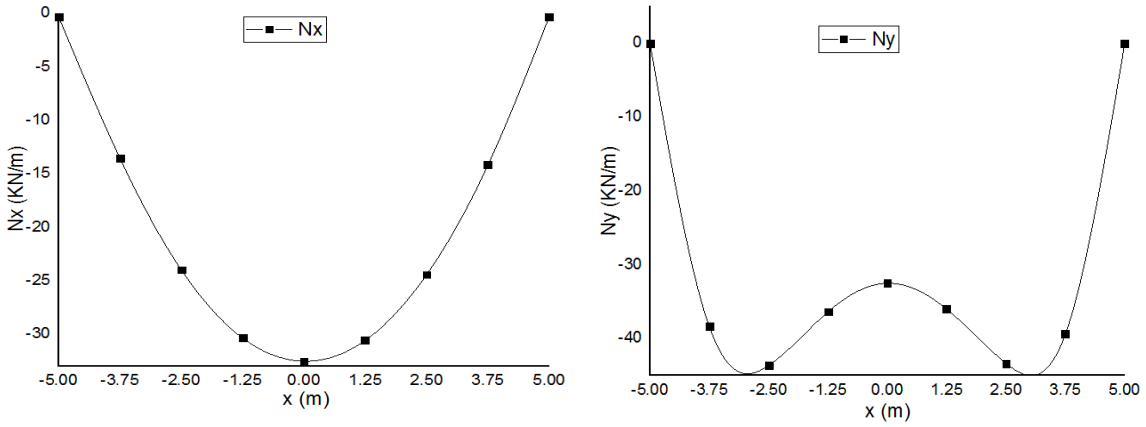

Figure 3-10: Internal force diagram by RFEM in the *x*-direction

Ny result in the central *y*-direction $N_y = -32.519\,kN/m$ at $x = 0.000m$ and $y = 0.000m$

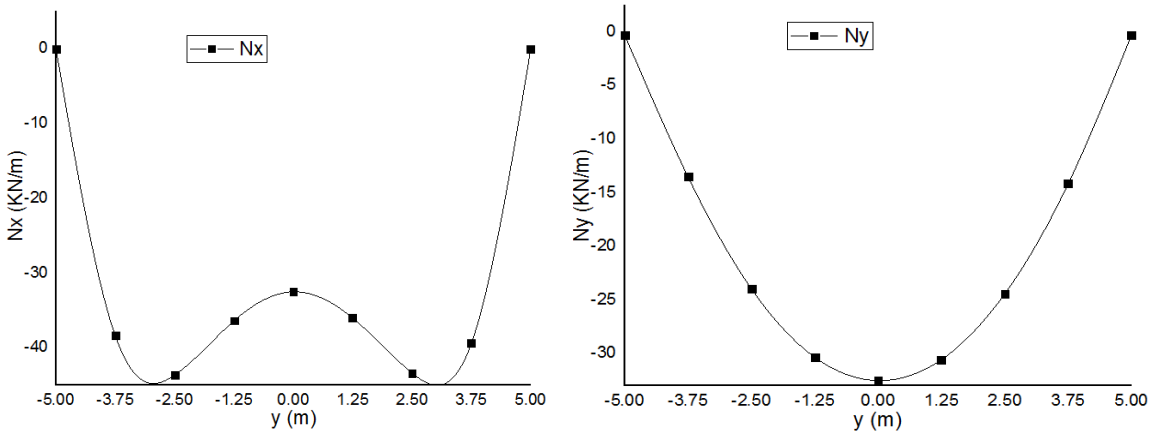

Figure 3-11: Internal force diagram by RFEM in the *y*-direction

Nxy result in the central *x* and *y* direction (*x* = 0.00m, *y* = -5.033m upto *x* = 0.000m, *y* = 5.033m and *x* = -5.033m, *y* = 0.000m upto *x* = 5.033m, *y* = 0.000m)

$$N_{xy} = 0.000\,kN/m \quad \text{at } x = 0.000m \text{ and } y = 0.000m$$

Nxy is zero in the central section of *y* and *x*-direction.

- Moment result in the central section

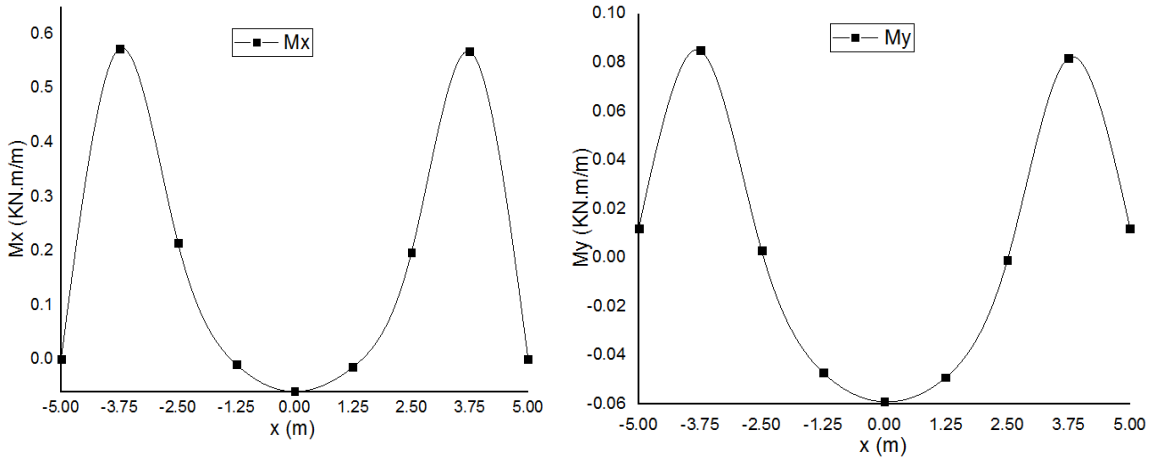

Figure 3-12: Moment diagram by RFEM in the *x*-direction

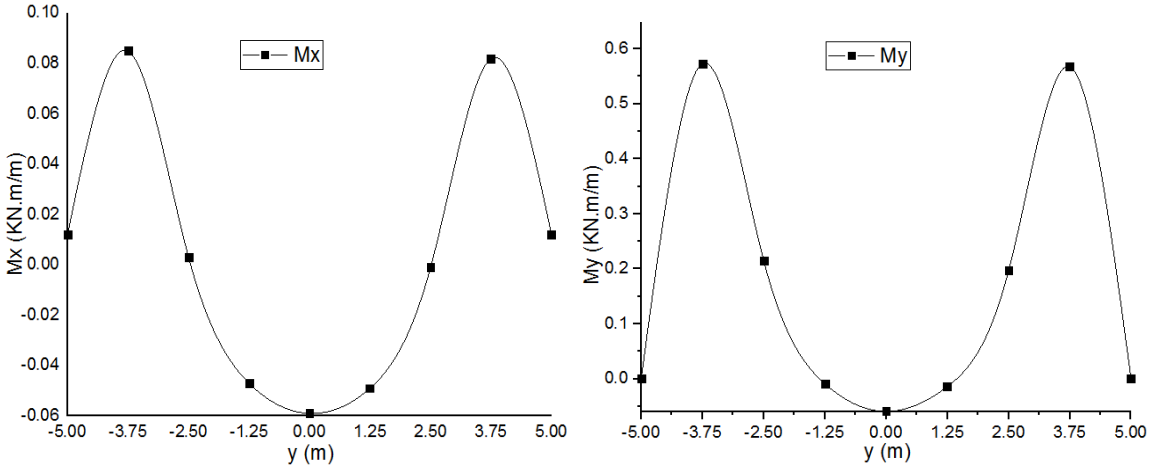

Figure 3-13: Moment diagram by RFEM in the *y*-direction

- Deformation

Deformation result in the central *x* and *y*-direction

$$\omega = 0.561mm \quad \text{at } x = 0.000m \text{ and } \quad y = 0.000m$$

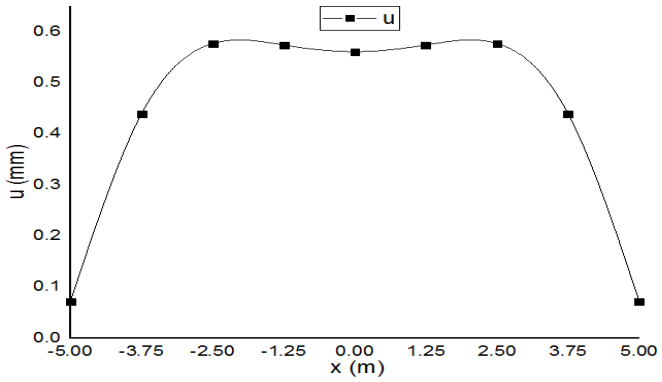

Figure 3-14: Deformation diagram by RFEM in *x* and *y*-direction

3.7 Comparing the Result of Theoretical and Numerical Analysis

Table 3-3: Theoretical and RFEM result

(a=5m, b=5m, f_1=0.5m, f_2=0.5m for C20/25)

					Computed by table		**Computed by RFEM**	
x/a	***y/b***	***x***	***y***	***K***	***Nx***	***Ny***	***Nx***	***Ny***
1.000	0.000	-5.000	0.000	1.020	0.000	-61.286	-0.293	-0.059
0.750	0.000	-3.750	0.000	1.011	-12.766	-49.323	-13.518	-38.404
0.500	0.000	-2.500	0.000	1.005	-22.863	-39.553	-23.970	-43.640
0.250	0.000	-1.250	0.000	1.001	-29.161	-33.333	-30.349	-36.382
0.000	0.000	0.000	0.000	1.000	-31.250	-31.250	-32.519	-32.520
0.250	0.000	1.250	0.000	1.001	-29.161	-33.333	-30.566	-36.023
0.500	0.000	2.500	0.000	1.005	-22.863	-39.553	-24.418	-43.370
0.750	0.000	3.750	0.000	1.011	-12.766	-49.323	-14.161	-39.412
1.000	0.000	5.000	0.000	1.020	0.000	-61.286	-0.293	-0.059
0.000	1.000	0.000	-5.000	0.981	-61.286	0.000	-0.059	-0.293
0.000	0.750	0.000	-3.750	0.989	-49.323	-12.766	-38.404	-13.518
0.000	0.500	0.000	-2.500	0.995	-39.553	-22.863	-43.640	-23.970
0.000	0.250	0.000	-1.250	0.999	-33.333	-29.161	-36.382	-30.349
0.000	0.000	0.000	0.000	1.000	-31.250	-31.250	-32.520	-32.519
0.000	0.250	0.000	1.250	0.999	-33.333	-29.161	-36.023	-30.566
0.000	0.500	0.000	2.500	0.995	-39.553	-22.863	-43.370	-24.418
0.000	0.750	0.000	3.750	0.989	-49.323	-12.766	-39.412	-14.161
0.000	1.000	0.000	5.000	0.981	-61.286	0.000	-0.059	-0.293

Table 3-4: DMV and RFEM result

(a=5m, b=5m, f_1=0.5m, f_2=0.5m for C20/25)

		Computed by (DMV) theory				**Computed by RFEM**			
x	***y***	***Nx***	***Ny***	***Mx***	***My***	***Nx***	***Ny***	***Mx***	***My***
0.000	5.000	0.000	0.000	0.000	0.000	-0.293	-0.059	0.000	0.012
1.250	5.000	-13.346	-38.360	0.565	0.096	-13.518	-38.404	0.573	0.085
2.500	5.000	-23.947	-43.394	0.204	0.008	-23.970	-43.640	0.215	0.003
3.750	5.000	-30.421	-36.205	-0.012	-0.046	-30.349	-36.382	-0.009	-0.047
5.000	5.000	-32.558	-32.558	-0.059	-0.059	-32.519	-32.520	-0.059	-0.059
6.250	5.000	-30.421	-36.205	-0.012	-0.046	-30.566	-36.023	-0.014	-0.049
7.500	5.000	-23.947	-43.394	0.204	0.008	-24.418	-43.370	0.197	-0.001
8.750	5.000	-13.346	-38.360	0.565	0.096	-14.161	-39.412	0.568	0.082
10.000	5.000	0.000	0.000	0.000	0.000	-0.293	-0.059	0.000	0.012
5.000	0.000	0.000	0.000	0.000	0.000	-0.059	-0.293	0.012	0.000
5.000	1.250	-38.360	-13.346	0.096	0.565	-38.404	-13.518	0.085	0.573
5.000	2.500	-43.394	-23.947	0.008	0.204	-43.640	-23.970	0.003	0.215
5.000	3.750	-36.205	-30.421	-0.046	-0.012	-36.382	-30.349	-0.047	-0.009
5.000	5.000	-32.558	-32.558	-0.059	-0.059	-32.520	-32.519	-0.059	-0.059
5.000	6.250	-36.205	-30.421	-0.046	-0.012	-36.023	-30.566	-0.049	-0.014
5.000	7.500	-43.394	-23.947	0.008	0.204	-43.370	-24.418	-0.001	0.197
5.000	8.750	-38.360	-13.346	0.096	0.565	-39.412	-14.161	0.082	0.568
5.000	10.000	0.000	0.000	0.000	0.000	-0.059	-0.293	0.012	0.000

Table 3-5: Deformation in the central section of a square elliptic parabolic shell

x	**DMV**	**RFEM**
	***u* (mm)**	***u* (mm)**
-5.000	0.000	0.072
-3.750	0.431	0.439
-2.500	0.561	0.577
-1.250	0.555	0.574
0.000	0.543	0.561
1.250	0.555	0.574
2.500	0.561	0.577
3.750	0.431	0.439
5.000	0.000	0.072

Table 3-6: Theoretical and RFEM result

(a=5m, b=4m, f_1=0.5m,f_2=0.4m for C20/25)

					Computed by table		**Computed by RFEM**	
x/a	***y/b***	***x***	***y***	***K***	***Nx***	***Ny***	***Nx***	***Ny***
1.000	0.000	-5.000	0.000	1.013	0.000	-39.498	-0.266	0.053
0.750	0.000	-3.750	0.000	1.007	-13.219	-33.043	-17.799	-31.557
0.500	0.000	-2.500	0.000	1.003	-23.983	-27.672	-30.872	-32.237
0.250	0.000	-1.250	0.000	1.001	-30.649	-24.301	-38.345	-24.673
0.000	0.000	0.000	0.000	1.000	-32.969	-23.120	-40.787	-21.399
0.250	0.000	1.250	0.000	1.001	-30.649	-24.301	-38.591	-24.355
0.500	0.000	2.500	0.000	1.003	-23.983	-27.672	-31.410	-31.859
0.750	0.000	3.750	0.000	1.007	-13.219	-33.043	-18.628	-32.233
1.000	0.000	5.000	0.000	1.013	0.000	-39.498	-0.266	0.053
0.000	1.000	0.000	-4.000	0.970	-75.792	0.000	-0.059	-0.295
0.000	0.750	0.000	-3.000	0.983	-58.512	-9.686	-33.282	-8.609
0.000	0.500	0.000	-2.000	0.992	-44.497	-17.173	-44.464	-15.458
0.000	0.250	0.000	-1.000	0.998	-35.868	-21.642	-42.898	-19.847
0.000	0.000	0.000	0.000	1.000	-32.969	-23.120	-40.793	-21.392
0.000	0.250	0.000	1.000	0.998	-35.868	-21.642	-42.722	-20.004
0.000	0.500	0.000	2.000	0.992	-44.497	-17.173	-44.579	-15.760
0.000	0.750	0.000	3.000	0.983	-58.512	-9.686	-34.416	-9.021
0.000	1.000	0.000	4.000	0.970	-75.792	0.000	-0.059	-0.295

Table 3-7: DMV and RFEM result

(a=5m, b=4m, f_1=0.5m,f_2=0.4m for C20/25)

		Computed by (DMV) theory				**Computed by RFEM**			
x	***y***	***Nx***	***Ny***	***Mx***	***My***	***Nx***	***Ny***	***Mx***	***My***
0.000	4.000	0.000	0.000	0.000	0.000	-0.266	0.053	0.000	0.012
1.250	4.000	-17.282	-30.413	0.346	0.014	-17.799	-31.557	0.459	0.060
2.500	4.000	-30.629	-30.707	0.092	-0.072	-30.872	-32.237	0.147	-0.013
3.750	4.000	-38.577	-25.125	0.022	-0.098	-38.345	-24.673	0.004	-0.047
5.000	4.000	-41.179	-23.077	0.022	-0.099	-40.787	-21.399	-0.016	-0.052
6.250	4.000	-38.577	-25.125	0.022	-0.098	-38.591	-24.355	0.002	-0.047
7.500	4.000	-30.629	-30.707	0.092	-0.072	-31.410	-31.859	0.134	-0.016
8.750	4.000	-17.282	-30.413	0.346	0.014	-18.628	-32.233	0.445	0.057
10.000	4.000	0.000	0.000	0.000	0.000	-0.266	0.053	0.000	0.012
5.000	0.000	0.000	0.000	0.000	0.000	-0.059	-0.295	-0.010	0.000
5.000	1.000	-32.805	-9.095	0.156	0.656	-33.282	-8.609	0.108	0.581
5.000	2.000	-44.531	-16.603	0.114	0.377	-44.464	-15.458	0.059	0.325
5.000	3.000	-43.224	-21.429	0.048	0.031	-42.898	-19.847	0.004	0.048
5.000	4.000	-41.179	-23.077	0.022	-0.099	-40.793	-21.392	-0.016	-0.052
5.000	5.000	-43.224	-21.429	0.048	0.031	-42.722	-20.004	0.002	0.038
5.000	6.000	-44.531	-16.603	0.114	0.377	-44.579	-15.760	0.056	0.308
5.000	7.000	-32.805	-9.095	0.156	0.656	-34.416	-9.021	0.107	0.576
5.000	8.000	0.000	0.000	0.000	0.000	-0.059	-0.295	-0.010	0.000

Table 3-8: Deformation in the central section of a rectangular elliptic parabolic shell

x	**DMV**	**RFEM**	***y***	**DMV**	**RFEM**
	***u* (mm)**	***u* (mm)**		***u* (mm)**	***u* (mm)**
-5.000	0	0.043	-4.000	0	0.071
-3.750	0.311	0.360	-3.000	0.361	0.377
-2.500	0.430	0.478	-2.000	0.501	0.479
-1.250	0.471	0.491	-1.000	0.501	0.497
0.000	0.484	0.490	0.000	0.484	0.490
1.250	0.471	0.491	1.000	0.501	0.497
2.500	0.430	0.480	2.000	0.501	0.482
3.750	0.311	0.372	3.000	0.361	0.349
5.000	0	0.043	4.000	0	0.071

3.8 Buckling Analysis

3.8.1 Theoretical Buckling Analysis

Material Properties;

- Young's modulus (E) = 30000 MPa
- Poisons ratio (μ) = 0.2
- The mass densities of the shell (ρ) = 2500 kg/m^3

Geometric Properties;

- Dimension: a = 10.0m and b = 10.0m
- Radius of curvature: R_1= 25.0m and R_2 = 25.0m
- The thickness of the elliptic parabolic shell: t =0.1m
- Raise of the shell: $f_1 = C_1$ = 0.5m and $f_2 = C_2$ = 0.5m

$$p_{cr} = \frac{2Et^2}{R_1 R_2 \sqrt{3\left(1-v^2\right)}}$$

where

E = Elastic modulus of concrete

t = Thickness of the shell

R_1 = Radius of curvature in the x-axis

R_2 = Radius of curvature in the y-axis

$$R_1 = \frac{1}{K_1} \text{ and } R_2 = \frac{1}{K_2}$$

where

K_1 = Curvature of the parabolic curve in the x-axis

K_2 = Curvature of the parabolic curve in the y-axis

$$K_1 = \frac{d^2z}{dx^2} = \frac{2f_1}{a^2} = \frac{2\times 0.5}{5^2} = \frac{1}{25} \text{ , } K_2 = \frac{d^2z}{dy^2} = \frac{2f_2}{b^2} = \frac{2\times 0.5}{5^2} = \frac{1}{25}$$

Equation of a parabolic curve derived from the general quadratic equation

$$z_x = ax^2 + bx + c \qquad \text{in the } x\text{-direction}$$

$$z_y = ay^2 + by + c \qquad \text{in the } y\text{-direction}$$

$$z_x = \frac{-x^2}{50} + 0.5$$

$$z_y = \frac{-y^2}{50} + 0.5$$

$$R_1 = 25m \; and \; R_2 = 25m \; at \; x = 0 \; and \; y = 0$$

$$p_{cr} = \frac{2Et^2}{R_1 R_2 \sqrt{3\left(1-v^2\right)}} = \frac{2\times 30\times 10^6 \times 0.1^2}{25\times 25\sqrt{3\left(1-0.2^2\right)}} = 565.685\, kN/m^2$$

3.8.2 DLUBAL RFEM Buckling Analysis

3.8.2.1 Add-on Module RF-STABILITY

The add-on module RF-STABILITY of the main program RFEM performs eigenvalue analyses for member and surface models to determine critical load factors and eigenvectors (buckling modes). The critical load factor (critical buckling load factor of the global system) allows you to evaluate the stability behavior of the structural system. The corresponding eigenvector indicates the region in the model that is prone to buckling [22].

3.8.2.2 Procedure for Analysis

Step 1. Create nodes at the required distance.
Step 2. Connect three nodes in the *x*, *y,* and *z*-direction by a parabola.
Step 3. Make a quadrangle (General four-sided surface) by selecting parabolic arches.
Step 4. Define the material property of the shell.
Step 5. Create the load case and apply a 1kN/m^2 uniformly distributed load.
Step 6. Add support around the shell surface. (Simply support around the surface)
Step 7. Generate finite element mesh
Step 8. Open adds on module stability then select RF stability.
Step 9. Analysis of the eigenvalue linear buckling.

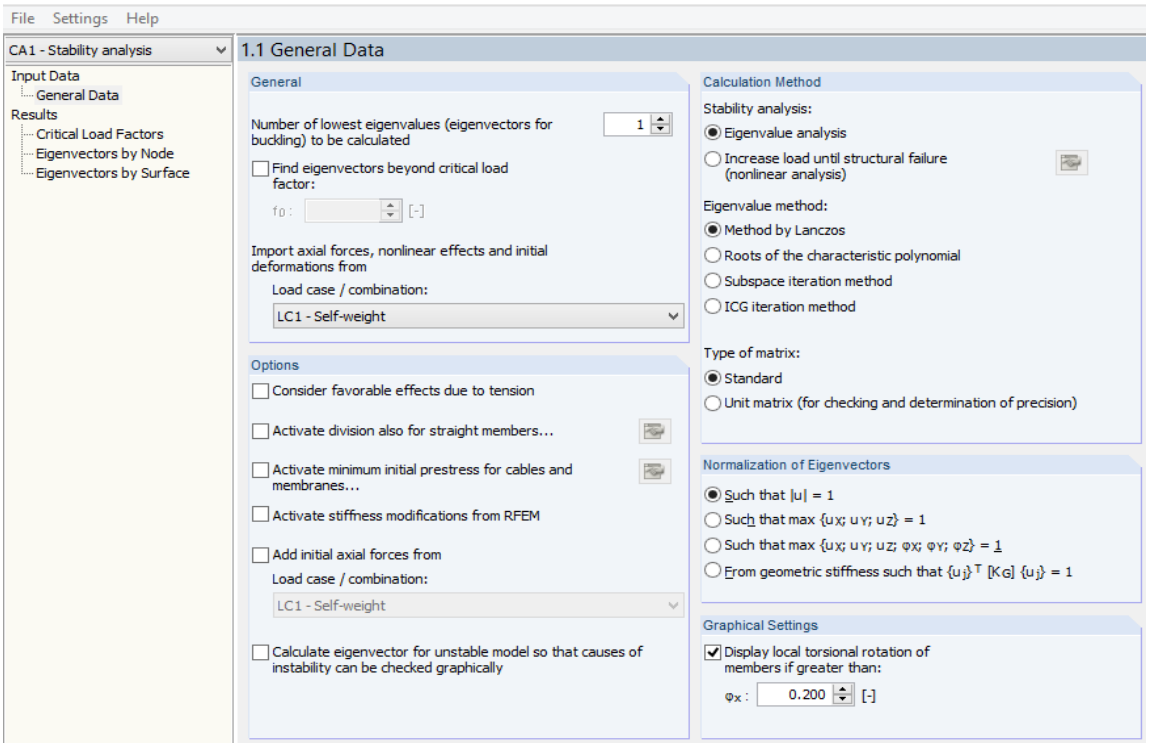

Figure 3-15: RF-STABILITY window 1.1 general data

As a result, RF-STABILITY yields a critical load factor of $570.418\,kN/m^2$

Table 3-9: Critical load factors

E-Value No.	Critical Load Factor	Magnification Factor
	f [-]	α [-]
1	570.418	1.002
2	570.418	1.002
3	591.803	1.002
4	593.345	1.002

$$p_{cr} = 565.685\,kN/m^2$$

The difference to the theoretical solution is thus about 0.837%

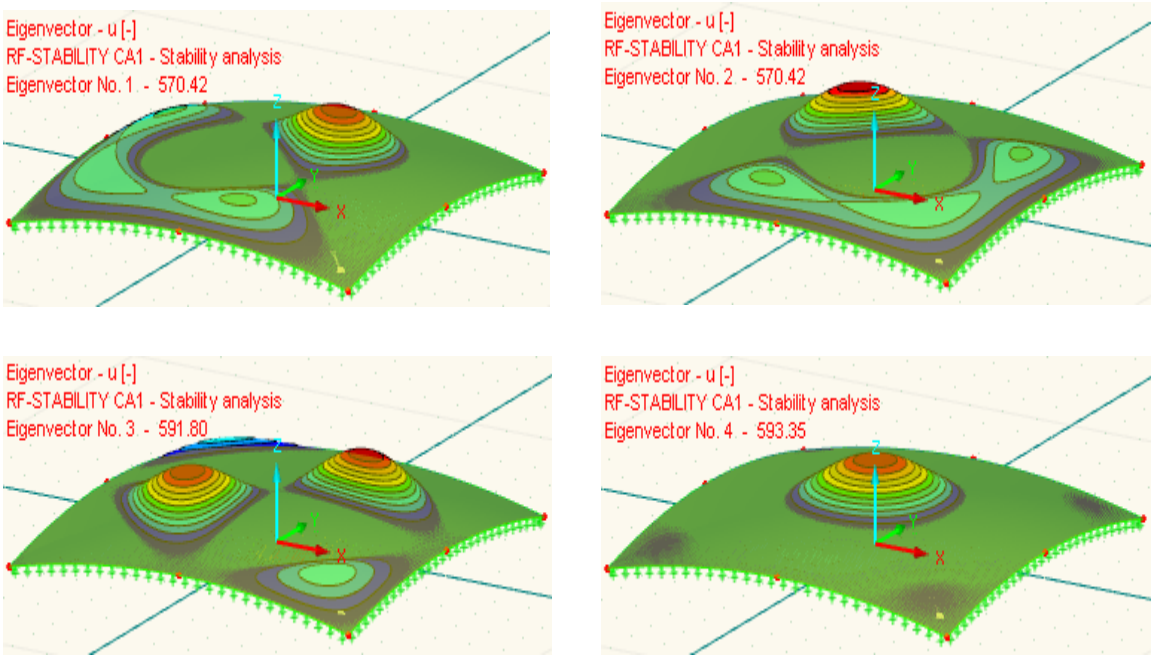

Figure 3-16: Mode shape with corresponding critical load

3.9 Critical Buckling Load with Varying Parameters

Table 3-10: Critical load with parameters 1

(a=b=5.0m, f_1=f_2=0.5m and R_1=R_2=25.0m)

Concrete Type	C20/25		C40/50		C60/75		
Thickness (m)	Pcr RFEM	Pcr	Pcr RFEM	Pcr	Pcr RFEM	Pcr	Difference in %
0.050	139.320	141.421	162.540	164.992	181.116	183.848	-1.486
0.060	201.938	203.647	235.594	237.588	262.519	264.741	-0.839
0.070	276.426	277.186	322.497	323.384	359.354	360.342	-0.274
0.080	360.722	362.039	420.842	422.378	468.939	470.650	-0.364
0.090	457.000	458.205	533.167	534.573	594.100	595.667	-0.263
0.100	570.418	565.685	665.488	659.966	741.543	735.391	0.837
0.110	701.689	684.479	818.637	798.559	912.196	889.823	2.514
0.120	825.676	814.587	963.289	950.352	1073.379	1058.963	1.361
0.130	958.761	956.008	1118.555	1115.343	1246.389	1242.811	0.288
0.140	1105.987	1108.743	1290.318	1293.534	1437.783	1441.366	-0.249
0.150	1268.845	1272.792	1480.319	1484.924	1649.499	1654.630	-0.310

Table 3-11: Critical load with parameters 2

(a=b=5.0m, f_1=f_2=0.6m and R_1=R_2=20.8m)

Concrete Type	C20/25		C40/50		C60/75		
Thickness (m)	Pcr RFEM	Pcr	Pcr RFEM	Pcr	Pcr RFEM	Pcr	Difference in %
0.050	198.360	203.647	231.420	237.588	257.868	264.741	-2.596
0.060	285.081	293.251	332.595	342.127	370.605	381.227	-2.786
0.070	389.728	399.148	454.683	465.672	506.646	518.892	-2.360
0.080	515.608	521.336	601.543	608.225	670.290	677.736	-1.099
0.090	652.946	659.815	761.770	769.785	848.830	857.760	-1.041
0.100	801.708	814.587	935.326	950.352	1042.220	1058.963	-1.581
0.110	973.494	985.650	1135.743	1149.925	1265.542	1281.345	-1.233
0.120	1170.233	1173.005	1365.272	1368.506	1521.303	1524.907	-0.236
0.130	1392.759	1376.652	1624.886	1606.094	1810.587	1789.648	1.170
0.140	1614.819	1596.591	1883.956	1862.689	2099.265	2075.568	1.142
0.150	1832.957	1832.821	2138.450	2138.291	2382.844	2382.667	0.007

Table 3-12: Critical load with parameters 3

(a=b=5.0m, f_1=f_2=0.7m and R_1=R_2=17.9m)

Concrete Type	C20/25		C40/50		C60/75		
Thickness (m)	Pcr RFEM	Pcr	Pcr RFEM	Pcr	Pcr RFEM	Pcr	Difference in %
0.050	261.564	277.186	305.158	323.384	340.033	360.342	-5.636
0.060	383.117	399.148	446.970	465.672	498.052	518.892	-4.016
0.070	519.789	543.284	606.421	633.832	675.726	706.270	-4.325
0.080	681.068	709.596	794.579	827.862	885.388	922.475	-4.020
0.090	874.590	898.082	1020.355	1047.763	1136.967	1167.507	-2.616
0.100	1083.177	1108.743	1263.707	1293.534	1408.130	1441.366	-2.306
0.110	1304.419	1341.580	1521.822	1565.176	1695.745	1744.053	-2.770
0.120	1549.970	1596.591	1808.298	1862.689	2014.961	2075.568	-2.920
0.130	1827.634	1873.776	2132.240	2186.072	2375.924	2435.909	-2.463
0.140	2139.533	2173.137	2496.122	2535.327	2781.393	2825.078	-1.546
0.150	2486.824	2494.673	2901.295	2910.452	3232.871	3243.075	-0.315

Table 3-13: Critical load with parameters 4

(a=b=5.0m, f_1=f_2=0.8m and R_1=R_2=15.6m)

Concrete Type	C20/25		C40/50		C60/75		
Thickness (m)	Pcr RFEM	Pcr	Pcr RFEM	Pcr	Pcr RFEM	Pcr	Difference in %
0.050	334.245	362.039	389.953	422.378	434.519	470.650	-7.677
0.060	482.958	521.336	563.451	608.225	627.845	677.736	-7.361
0.070	667.339	709.596	778.562	827.862	867.541	922.475	-5.955
0.080	870.311	926.819	1015.363	1081.289	1131.4	1204.865	-6.097
0.090	1104.19	1173.005	1288.216	1368.506	1435.44	1524.907	-5.867
0.100	1378.51	1448.155	1608.264	1689.514	1792.07	1882.601	-4.809
0.110	1688.94	1752.267	1970.429	2044.312	2195.62	2277.947	-3.614
0.120	1999.77	2085.343	2333.063	2432.900	2599.7	2710.946	-4.104
0.130	2335.94	2447.381	2725.268	2855.278	3036.73	3181.596	-4.553
0.140	2711.28	2838.383	3163.154	3311.447	3524.66	3689.898	-4.478
0.150	3128.9	3258.348	3650.388	3801.406	4067.58	4235.852	-3.973

Table 3-14: Critical load with parameters 5

(a=5.0m, b=4m, f_1=0.7m, f_2=0.5m, R_1=17.9m and R_2=16.0m)

Concrete Type	C20/25		C40/50		C60/75		
Thickness (m)	Pcr RFEM	Pcr	Pcr RFEM	Pcr	Pcr RFEM	Pcr	Difference in %
0.050	277.112	309.359	323.297	360.919	360.246	402.167	-10.424
0.060	408.852	445.477	476.994	519.723	531.508	579.120	-8.222
0.070	550.178	606.344	641.874	707.401	715.231	788.247	-9.263
0.080	719.022	791.960	838.859	923.953	934.729	1029.547	-9.210
0.090	922.877	1002.324	1076.690	1169.378	1199.740	1303.021	-7.926
0.100	1166.147	1237.437	1360.505	1443.676	1515.991	1608.668	-5.761
0.110	1429.340	1497.299	1667.563	1746.848	1858.142	1946.488	-4.539
0.120	1678.715	1781.909	1958.501	2078.894	2182.330	2316.482	-5.791
0.130	1958.293	2091.268	2284.675	2439.813	2545.781	2718.649	-6.359
0.140	2270.663	2425.376	2649.107	2829.606	2951.862	3152.989	-6.379
0.150	2618.263	2784.233	3054.640	3248.272	3403.742	3619.503	-5.961

Table 3-15: Critical load with parameters 6

(a=5.0m, b=4m, f_1=0.8m, f_2=0.5m, R_1=15.6m and R_2=16.0m)

Concrete Type	C20/25		C40/50		C60/75		
Thickness (m)	Pcr RFEM	Pcr	Pcr RFEM	Pcr	Pcr RFEM	Pcr	Difference in %
0.050	333.674	353.553	389.286	412.479	433.776	459.619	-5.623
0.060	477.440	509.117	557.013	593.970	620.672	661.852	-6.222
0.070	659.587	692.965	769.518	808.459	857.463	900.854	-4.817
0.080	854.373	905.097	996.769	1055.946	1110.685	1176.626	-5.604
0.090	1081.436	1145.513	1261.675	1336.432	1405.867	1489.167	-5.594
0.100	1349.776	1414.214	1574.739	1649.916	1754.709	1838.478	-4.556
0.110	1640.922	1711.198	1914.409	1996.398	2133.199	2224.558	-4.107
0.120	1933.931	2036.468	2256.253	2375.879	2514.110	2647.408	-5.035
0.130	2263.195	2390.021	2640.394	2788.358	2942.154	3107.027	-5.306
0.140	2631.750	2771.859	3070.375	3233.835	3421.275	3603.416	-5.055
0.150	3042.484	3181.981	3549.565	3712.311	3955.229	4136.575	-4.384

3.10 Free Vibration Analysis

3.10.1 Rectangular Plan Elliptic Parabolic Shell

The geometric and material properties of the elliptic parabolic shell given below.

Material Properties;

- Young's Modulus (E) = 30000 MPa
- Poisons Ratio (μ) = 0.2
- The mass densities of the shell (ρ) = 2500 kg/m^3

Geometric Properties;

- Dimension: a = 10.0m and b = 8.0m
- Radius of curvature: R_1= 25.0m and R_2 = 20.0m
- Thickness of the elliptic parabolic shell : h = 0.1m
- Raise of the shell: f_1 = 0.5m and f_2 = 0.4m

Firstly, calculate the value of λ_n and μ_m . where $m = n = 1$

$$\lambda_1 = \frac{\pi}{a} = \frac{\pi}{10m} = 0.314/m$$

$$\mu_1 = \frac{\pi}{b} = \frac{\pi}{8m} = 0.393/m$$

$$D = \frac{Eh^3}{12(1-v^2)} = \frac{30 \times 10^9\, N/m^2 \times (0.1m)^3}{12(1-0.2^2)} = 2{,}604{,}166.667\ N.m$$

$$\omega_{11}^2 = \frac{1}{\rho h}\left[D\left(\lambda_1^2+\mu_1^2\right)^2 + \frac{Eh\left(\frac{\lambda_1^2}{R_1}+\frac{\mu_1^2}{R_2}\right)^2}{\left(\lambda_1^2+\mu_1^2\right)^2} \right]$$

$$\omega_{11}^2 = \frac{1}{2500\times 0.1 kg/m^2}\left[\begin{array}{l} 2{,}604{,}166.667 N.m\left(0.314^2/m^2+0.393^2/m^2\right)^2 \\ +\dfrac{30\times 10^8\, N/m\times 0.1m\left(\dfrac{0.314^2/m^2}{25m}+\dfrac{0.393^2/m^2}{20m}\right)^2}{\left(0.314^2/m^2+0.393^2/m^2\right)^2} \end{array} \right]$$

$$\omega_{11}^2 = \frac{1}{250\, kg/m^2}\left[2{,}604{,}166.667 N.m\times 0.064/m^4 + \frac{30\times 10^8 N\times 0.000123382/m^6}{0.064/m^4} \right]$$

$$\omega_{11}^2 = \frac{1}{250\, kg/m^2}\left[166{,}570.312\, N/m^3 + 5{,}782{,}253.073\, N/m^3 \right]$$

$$\omega_{11}^2 = 23{,}795.294\left(rad/s\right)^2$$

$$\omega_{11} = 154.257\ rad/s$$

Natural frequency

$$f_n = \frac{\omega_{11}}{2\pi} = \frac{154\, rad/s}{2\pi} = 24.550 Hz$$

Natural Period

$$t_n = \frac{2\pi}{\omega_{11}} = \frac{2\pi}{154\, rad/s} = 0.040 s$$

3.10.2 DLUBAL RFEM Analysis

3.10.2.1 RF DYNAM

With the add-on module RF-/DYNAM - natural vibrations, it is possible to quickly analyze conveniently natural frequencies and mode shapes for spatial member models.

The natural vibration cases tab is the centerpiece of the RF-DYNAM Pro - natural vibrations module. It is essential for the response spectrum analysis and the time history analysis based on modal decomposition (modal analysis) [23].

The equation of motion of a multi-degree of freedom without damping is solved with the four available eigenvalue solvers. The equation of motion is defined as

$$M\ddot{u} + Ku = 0 \qquad 3\text{-}22$$

where M is the mass matrix, K is the stiffness matrix and u are he mode shapes containing translational and rotational parts:

$$u = \left(u_x, u_y, u_z, \varphi_x, \varphi_y, \varphi_z\right)^T \qquad 3\text{-}23$$

The eigenvalue λ [1/s2] is connected to the angular frequency ω [1/s] with $\lambda i = \omega i^2$. The natural frequency f [Hz] is then derived with $f = \omega/2\pi$, and the natural period t [s] is the reciprocal of the frequency obtained with $t = 1/f$.

Table 3-16: Eigenvalue, natural frequency and periods

E-vector	Eigenvalue	Angular Frequency	Natural Frequency	Natural Period
No.	λ [1/s^2]	ω [rad/s]	f [Hz]	t [s]
1	28810.147	169.736	27.014	0.037
2	36522.759	191.109	30.416	0.033
3	36677.769	191.514	30.480	0.033
4	39001.398	197.488	31.431	0.032
5	42468.679	206.079	32.799	0.030
6	52482.088	229.090	36.461	0.027

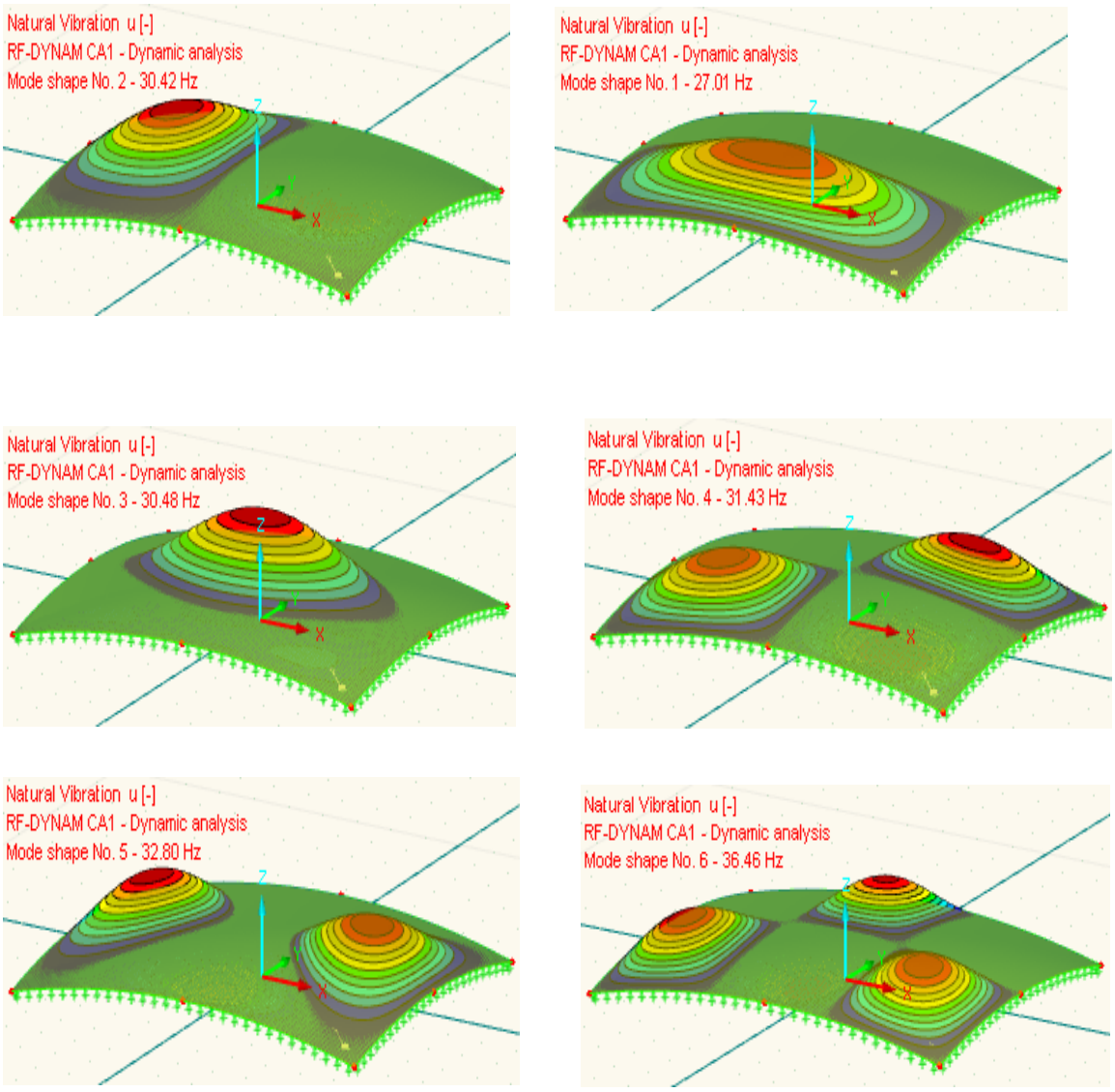

Figure 3-17: Mode shape with corresponding natural frequency (Hz)

Comparing the result of the elliptic parabolic shell during free (natural) vibration that is calculated by theoretically and by RFEM.

Table 3-17: Mode 1 result by theoretical and RFEM 1

C20/25							
Thick ness(m)	D (N.m)	Theoretical result			RFEM result		
		ω (rad/s)	f (Hz)	t (s)	ω (rad/s)	f (Hz)	t (s)
0.050	325520.833	152.629	24.292	0.041	157.269	25.030	0.040
0.060	562500.000	152.869	24.330	0.041	159.369	25.364	0.039
0.070	893229.167	153.152	24.375	0.041	161.631	25.724	0.039
0.080	1333333.333	153.478	24.427	0.041	164.105	26.118	0.038
0.090	1898437.500	153.847	24.485	0.041	166.806	26.548	0.038
0.100	2604166.667	154.257	24.551	0.041	169.736	27.014	0.037
0.110	3466145.833	154.710	24.623	0.041	172.887	27.516	0.036
0.120	4500000.000	155.205	24.702	0.040	176.252	28.051	0.036
0.130	5721354.167	155.740	24.787	0.040	179.820	28.619	0.035
0.140	7145833.333	156.317	24.879	0.040	183.581	29.218	0.034
0.150	8789062.500	156.934	24.977	0.040	187.522	29.845	0.034

3.10.3 Square Plan Elliptic Parabolic Shell

The same material property from the rectangular plan only the geometrical property varies.

Geometric Properties;

- Dimension: a = 10m and b = 10m
- Radius of curvature: R_1= 25m and R_2 = 25m
- Thickness of the elliptic parabolic shell : h = 0.05-0.15m
- Raise of the shell: f_1 = 0.5m and f_2 = 0.5m

Table 3-18: Mode 1 result by theoretical and RFEM 2

C20/25							
Thick ness(m)	D (N.m)	Theoretical result			RFEM result		
		ω (rad/s)	f (Hz)	t (s)	ω (rad/s)	f (Hz)	t (s)
0.050	325520.833	138.930	22.111	0.045	145.812	23.207	0.043
0.060	562500.000	139.090	22.137	0.045	148.886	23.696	0.042
0.070	893229.167	139.280	22.167	0.045	152.302	24.240	0.041
0.080	1333333.333	139.498	22.202	0.045	154.954	24.662	0.041
0.090	1898437.500	139.745	22.241	0.045	156.733	24.945	0.040
0.100	2604166.667	140.021	22.285	0.045	158.522	25.230	0.040
0.110	3466145.833	140.325	22.333	0.045	160.357	25.522	0.039
0.120	4500000.000	140.657	22.386	0.045	162.260	25.824	0.039
0.130	5721354.167	141.017	22.444	0.045	164.244	26.140	0.038
0.140	7145833.333	141.405	22.505	0.044	166.316	26.470	0.038
0.150	8789062.500	141.821	22.572	0.044	168.480	26.814	0.037

CHAPTER 4 RESULT AND DISCUSSION

4.1 Introduction

Results from the parametric study drawn in the previous chapter are obtainable. These results include the internal forces, critical buckling loads, and natural vibration during different parameters. The study also uses the graphical presentation to display the mode of buckling and natural vibration and the influence of fluctuation as one or two of the geometrical parameters changed. Some remarkable trends are observed when the results are plotted against the various geometrical parameters.

4.2 Internal Forces

When compared to the result of internal forces obtained from theoretical and finite element analysis in the elliptic paraboloid thin shell model.

- For square plan elliptic paraboloid shell

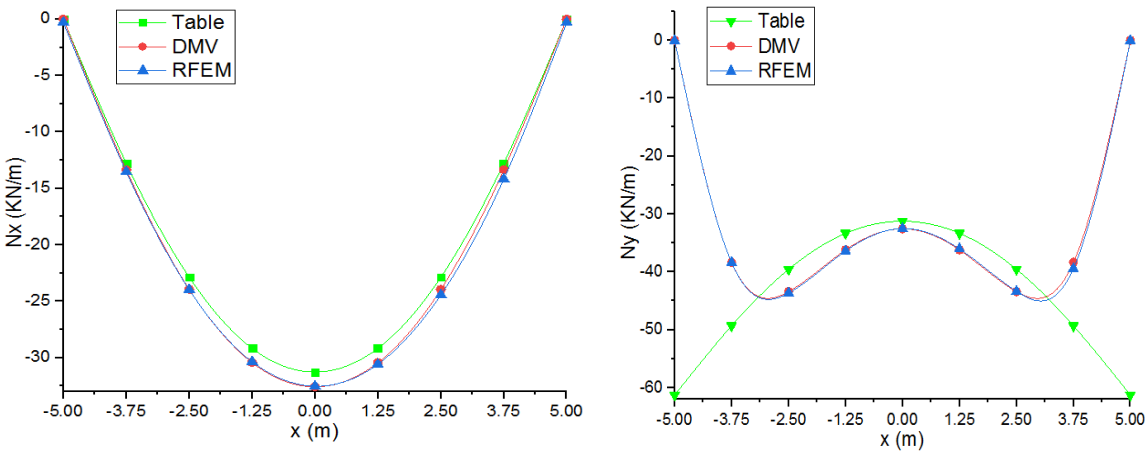

Figure 4-1: Comparing internal force in the central section in the *x*-direction

The value of *Nx* in the *x*-direction of the elliptic parabolic shell obtained nearly the same curve from two theoretically obtained formulas and finite element software but *Ny* value is nearly the same by DMV (shallow shell theory) and finite element software only.

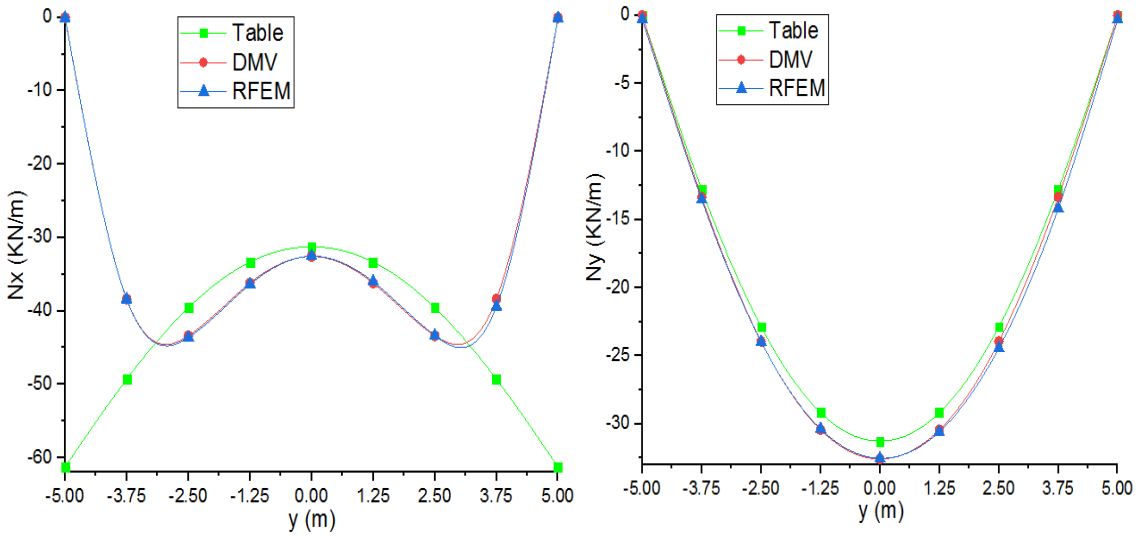

Figure 4-2: Comparing internal force in the central section in the *y*-direction

The value of *Ny* in the *y*-direction of the elliptic parabolic shell obtained nearly the same curve from two theoretically obtained formulas and finite element software but *Nx* value by DMV (shallow shell theory) is closely similar to finite element software only.

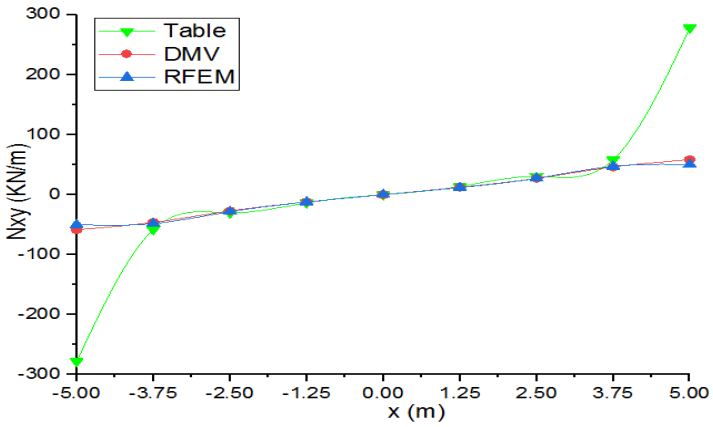

Figure 4-3: Comparing *Nxy* in the *x* and *y*-direction around the edge

Shear *Nxy* for the square elliptic parabolic shell is the same in *x* and y-direction but the values obtained from theoretical and finite elements are equivalent around the edge except at the corner. The table of coefficients theoretically based formula gives higher shear force than the shallow shell theory and finite element method.

- For rectangular plan elliptic paraboloid shell

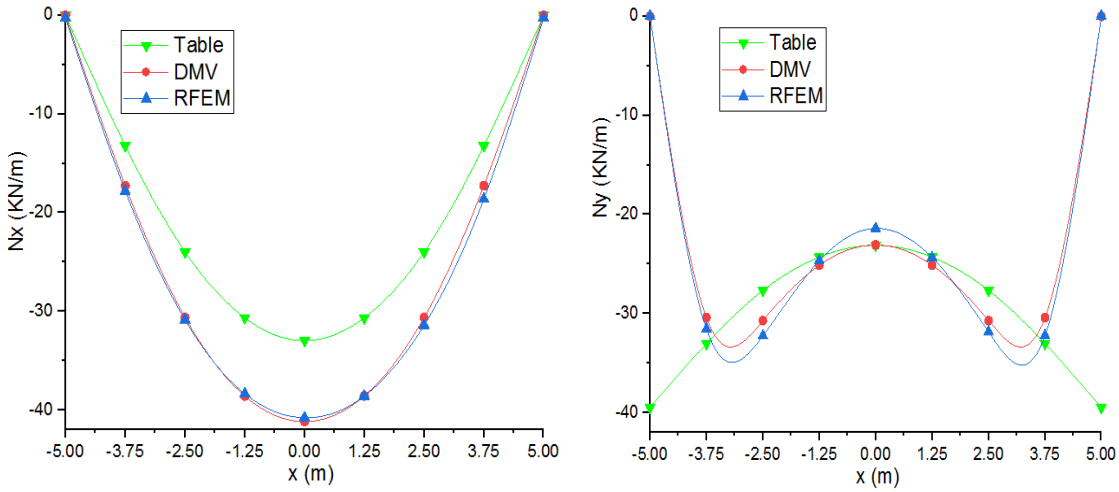

Figure 4-4: Comparing internal force in the central section in the *x*-direction

Internal force *Nx* is higher at the center of the shell but *Ny* higher near to the edge and values obtained from DMV and the finite element is equivalent in the *x*-direction.

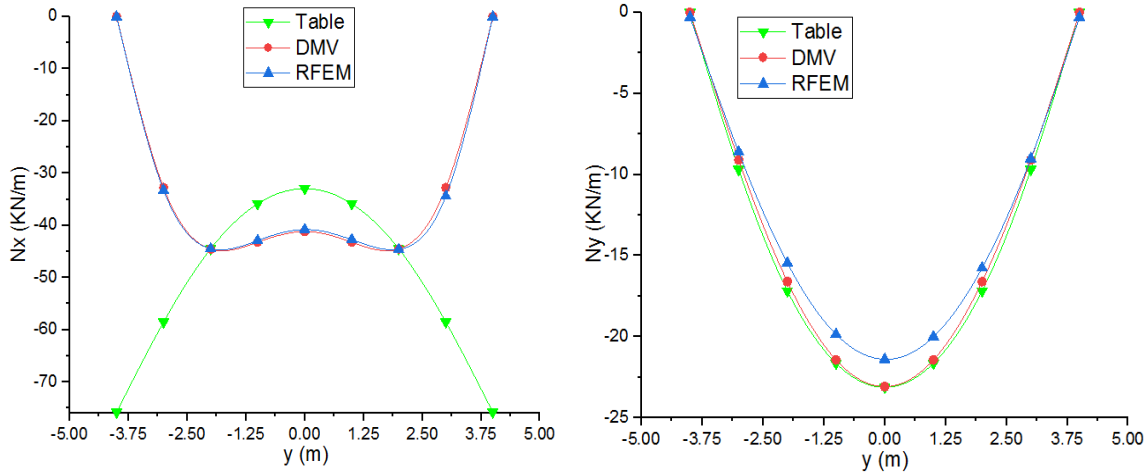

Figure 4-5: Comparing internal force in the central section in the *y*-direction

From the diagram, it has been observed that *Nx* values determined by DMV and RFEM are identical in the other way *Ny* results obtained by a table of coefficient and DMV are similar.

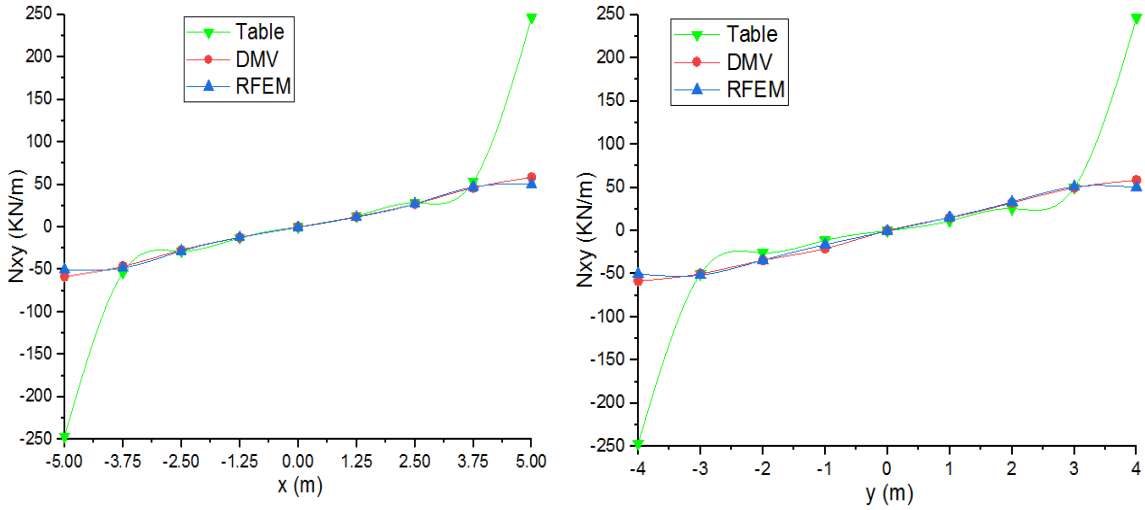

Figure 4-6: Comparing *Nxy* in the *x* and *y*-direction around the corner

Nxy values in the rectangular and square plan elliptic parabolic shell show that at the corner is higher than at the edge in the *x* and *y*-direction.

4.3 Moment

In this research paper, it has compared the moment results obtained by the shallow shell theory and finite element software (RFEM) for rectangular and square elliptic parabolic shell.

- For square plan elliptic paraboloid shell

Figures 4-7 and 4-8 show the value of *Mx* and *My* value interchangeable in the *x* and *y*-direction and equal. *Mxy* is in the same pattern and higher at the corner by DMV.

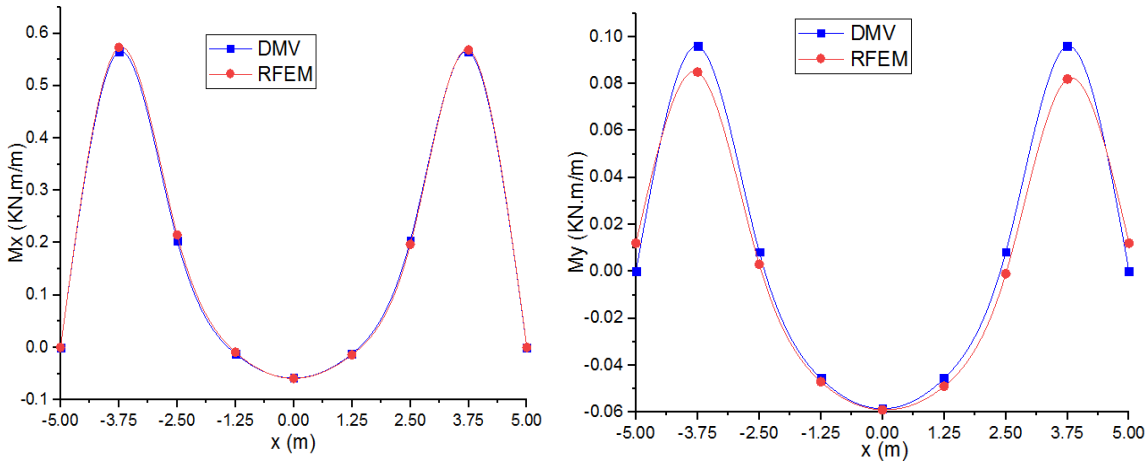

Figure 4-7: Comparing moment in the central section in the *x*-direction

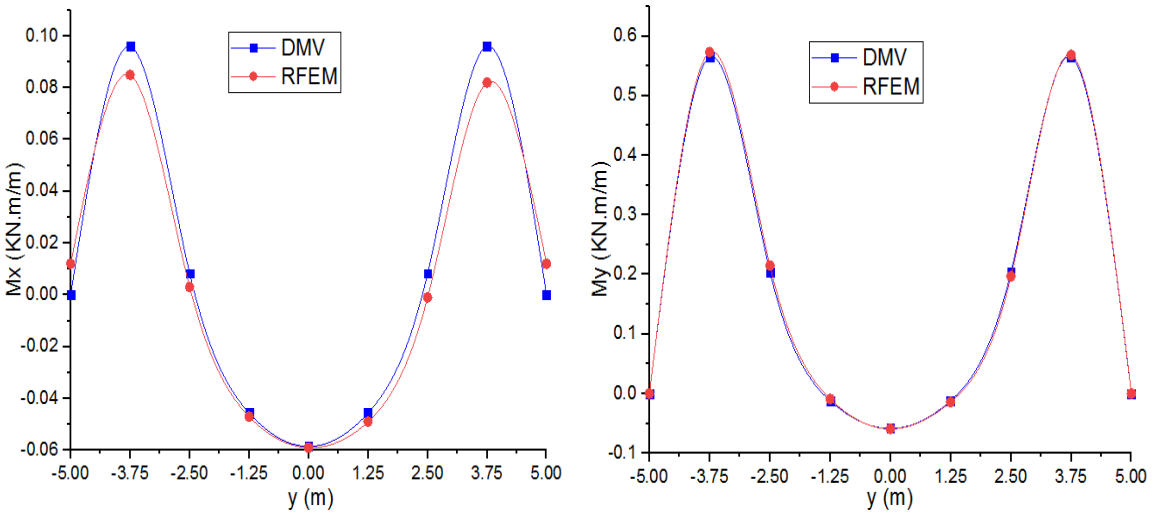

Figure 4-8: Comparing moment in the central section in the *y*-direction

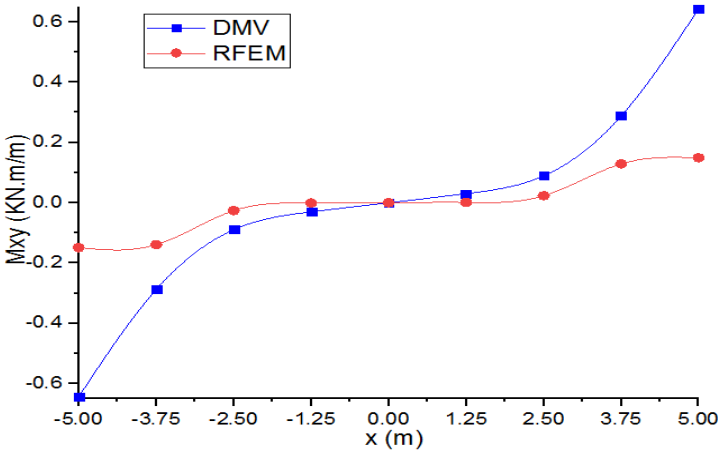

Figure 4-9: Comparing *Mxy* in the *x* and *y*-direction around the edge

- For rectangular plan elliptic paraboloid shell

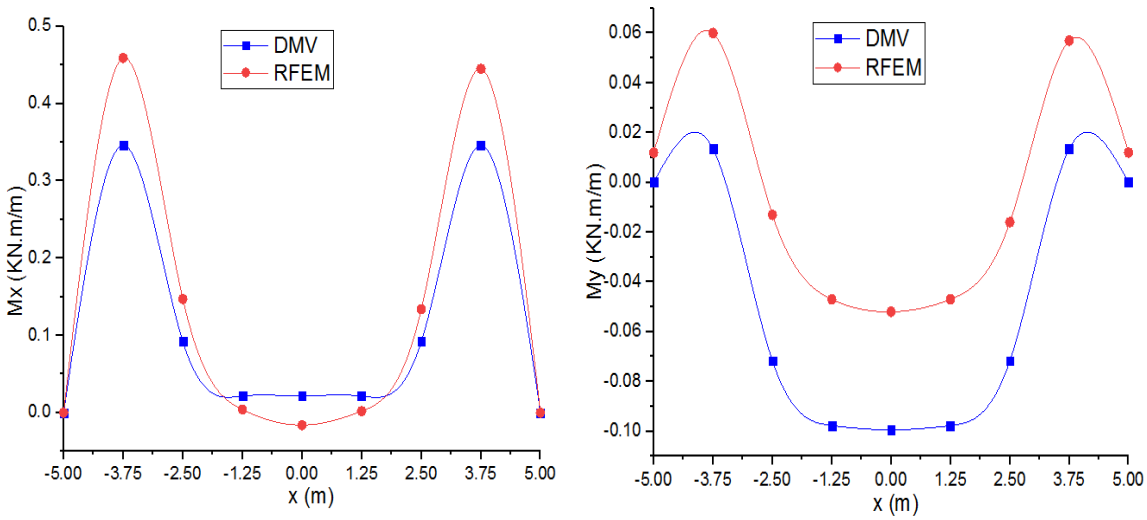

Figure 4-10: Comparing moment in the central section in the *x*-direction

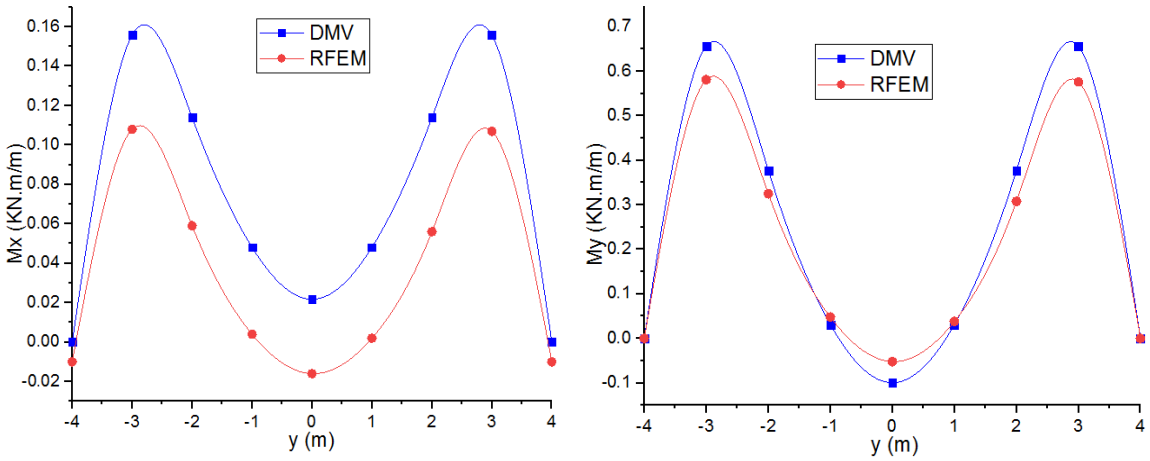

Figure 4-11: Comparing moment in the central section in the *y*-direction

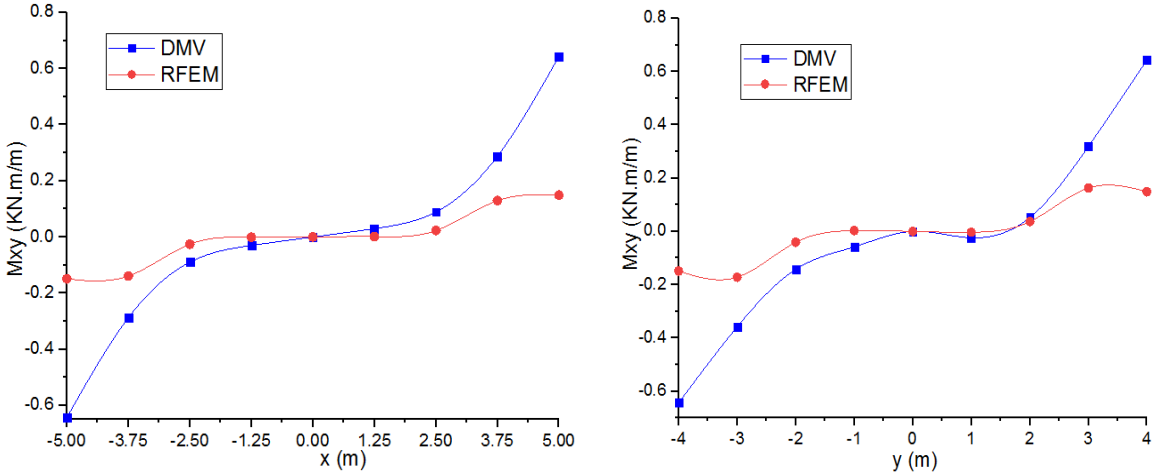

Figure 4-12: Comparing *Mxy* in the *x* and *y*-direction

4.4 Deformation

- For square plan elliptic paraboloid shell

The deformation result obtained from both theoretical and RFEM methods is almost similar in the central section of the shell. The deformation near the edge is negligible.

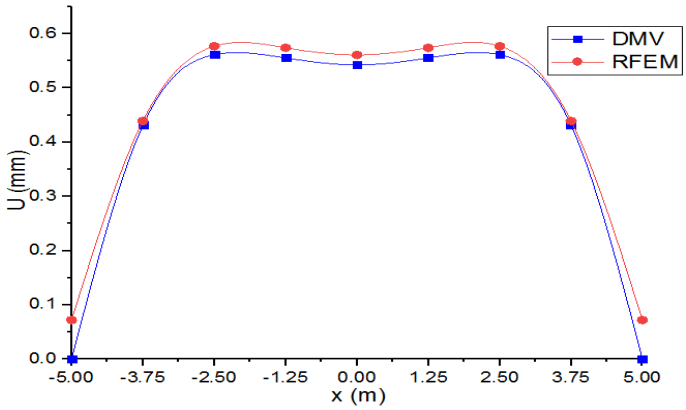

Figure 4-13: Deformation in the central section x and y-direction

- For rectangular plan elliptic paraboloid shell

Figure 4-14 shows the deformation of the rectangular plan elliptic parabolic shell is zero near the edge and increased highly goes to the center.

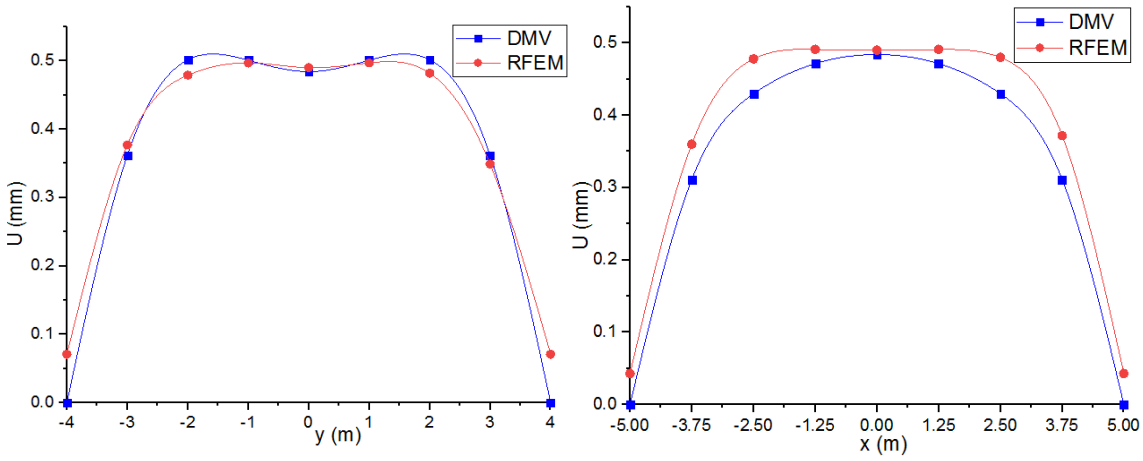

Figure 4-14: Deformation in the central section of the rectangular plan shell

4.5 Critical Buckling Load

The percentile variation of the value of the critical buckling load of the shell that is done by theoretically and numerically is increased when the shallowness of the shell is increased in square plan elliptic parabolic shell with the thickness of the shell is (5 – 15cm) this is seen in the graph. The term shallowness means the side raise of the elliptic paraboloid shells.

The relation between buckling load and radius of curvature of the shell is inversely this is clearly shown in the result that gained by both analysis methods. When the radius of curvature decreased from 25m to 15.625m in the opposite way the critical buckling load increased 139.320 to 334.245 kN/m^2.

For a rectangular shell, the percentile difference of the critical buckling load is varied when the shallowness of the shell is increased.

In general, the shallowness, the radius of curvature, type of concrete, and thickness of the shell has a significant impact on the critical buckling load of the shell.

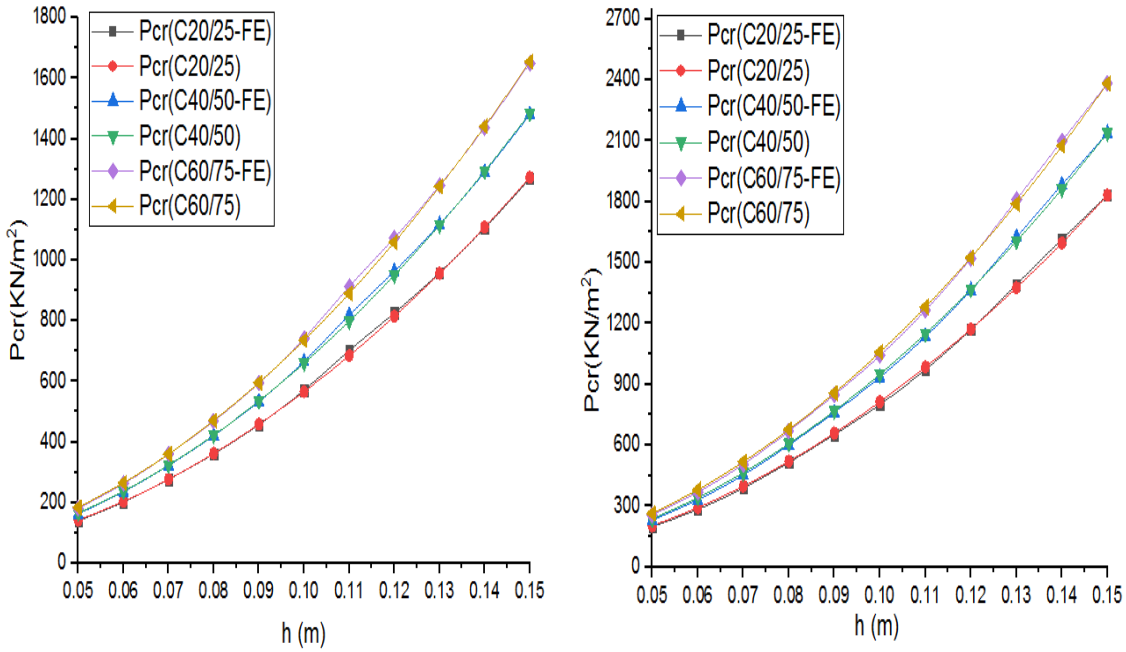

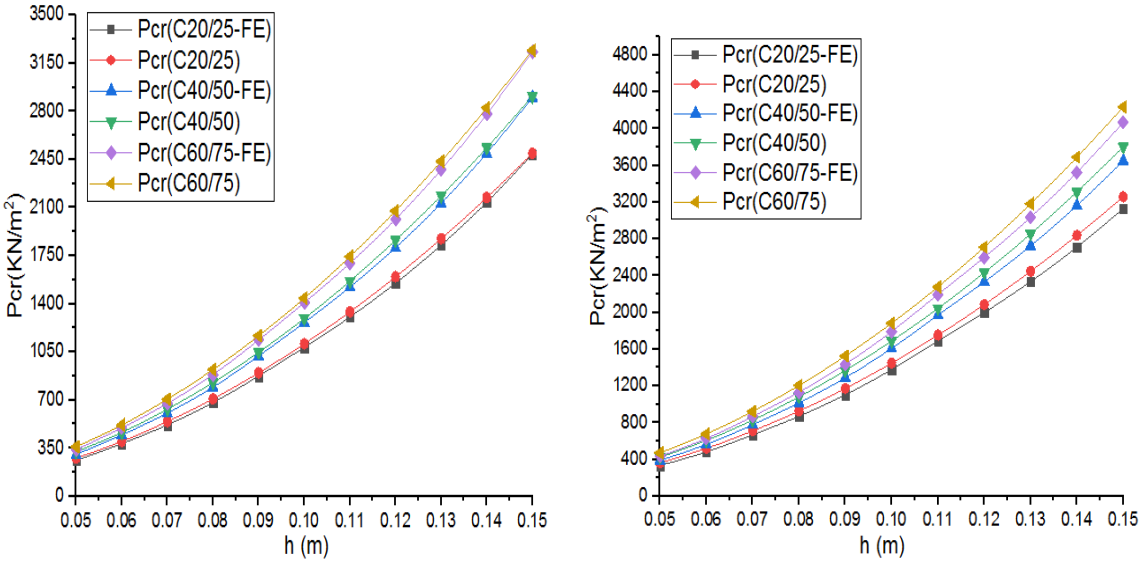

Figure 4-15: Buckling of square plan elliptic paraboloid shell with varying shallowness and thickness

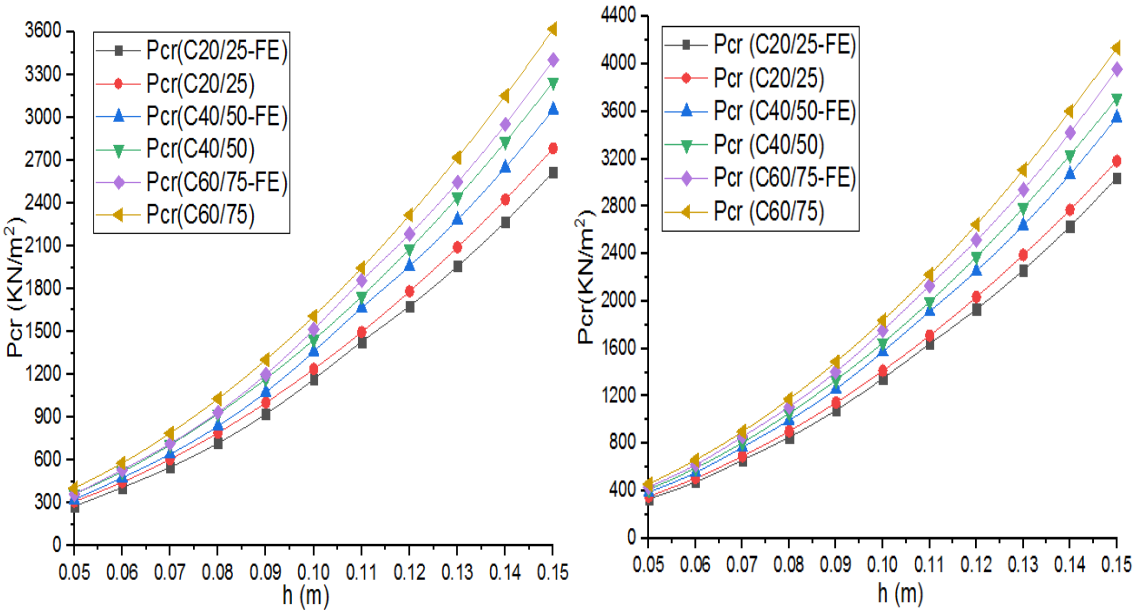

Figure 4-16: Buckling of rectangular plan elliptic paraboloid shell with varying shallowness and thickness

4.6 Free Vibration of the Shell

For both rectangular and squared plan elliptic paraboloid shell the value of angular frequency, natural frequency, and period that is obtained by theoretical and numerical has a small difference when the shell is thinnest (5cm). On the other way, the values of geometrical parameters that are thickness increased the natural and angular frequency also increased but the finite element software gives a higher value than the theoretical one.

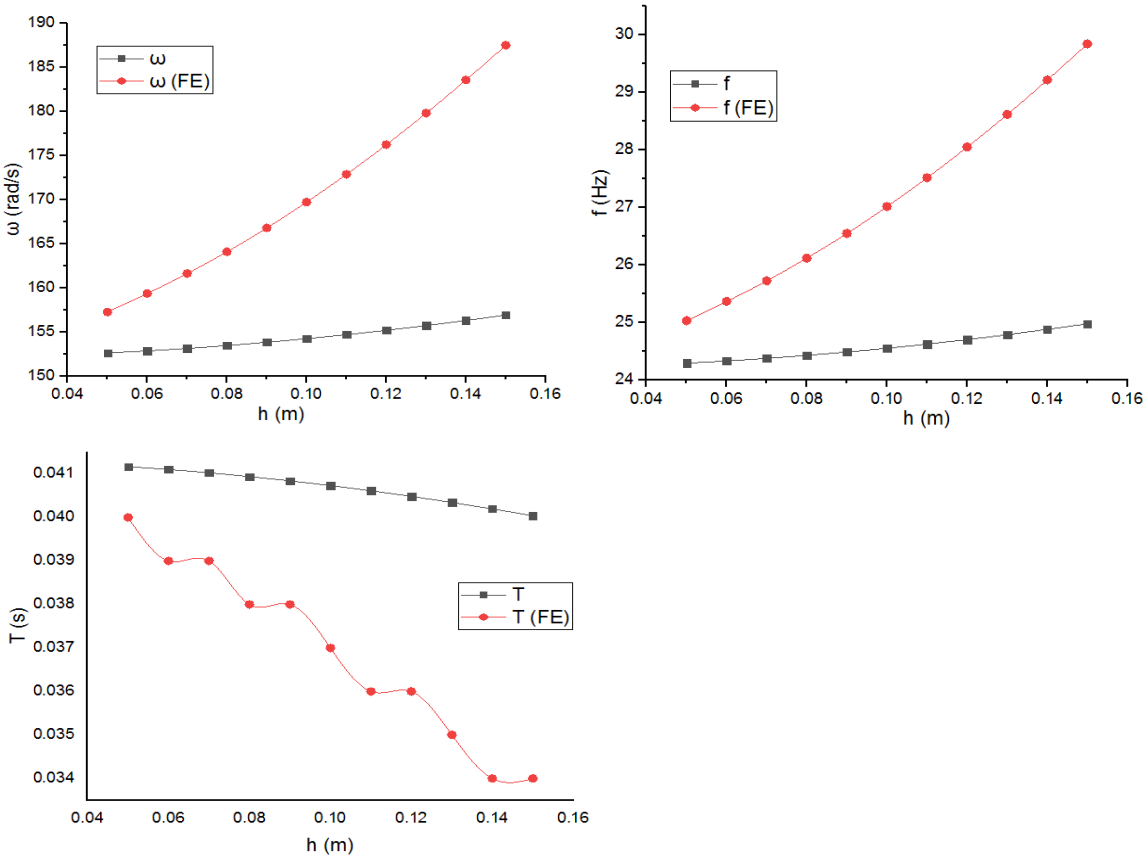

Figure 4-17: Free vibration results for rectangular plan elliptic paraboloid

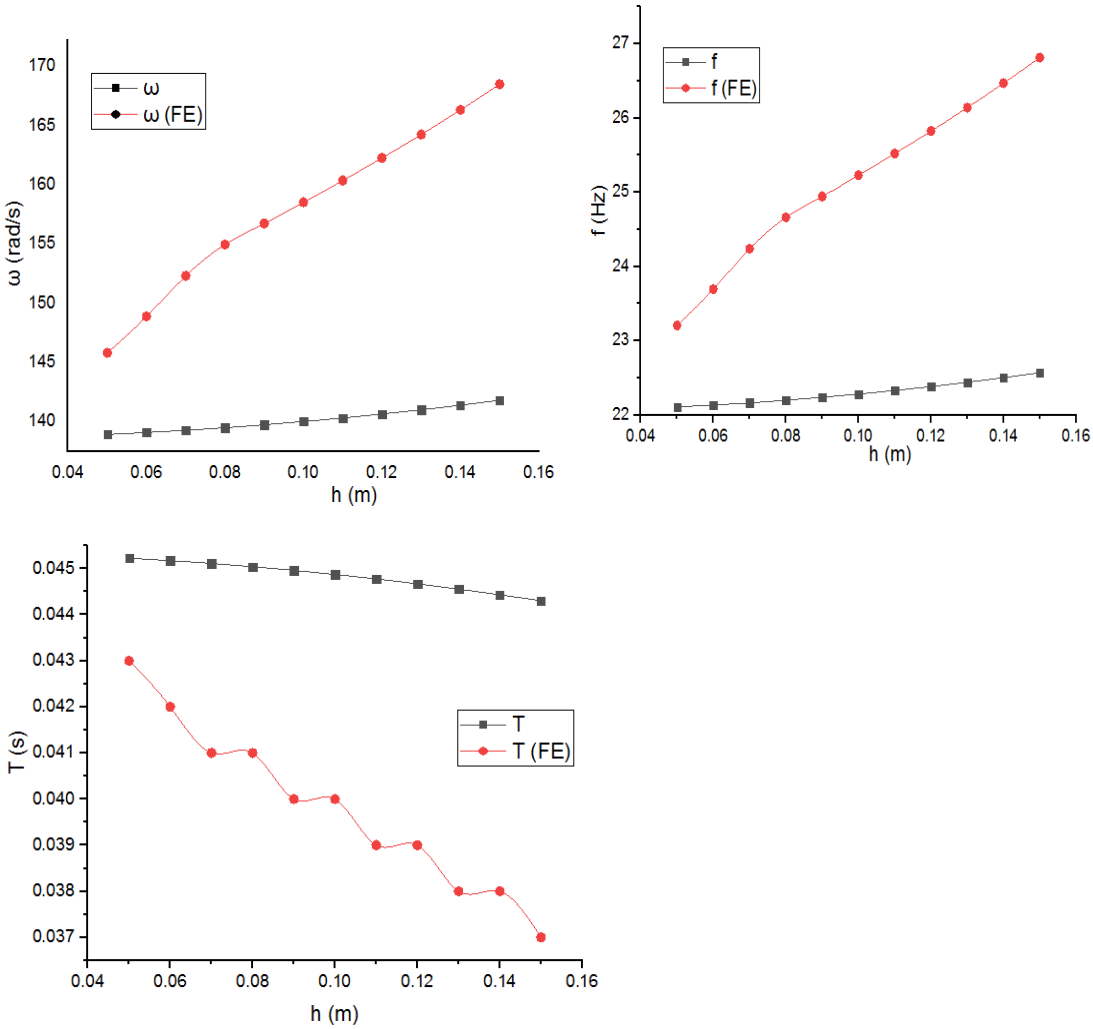

Figure 4-18: Free vibration results for square plan elliptic paraboloid

CHAPTER 5 CONCLUSIONS AND RECOMMENDATIONS

5.1 Conclusions

This research is mainly focused on the parametric study on the stability of a thin concrete shell by its own weight. The conclusion derived from the results obtained by analyzing the model of the elliptic paraboloid shells. The geometrical and material parameters were changed in the analysis of critical buckling load to obtain the relationships between thickness, elastic modulus, and radius of curvature. From the parameters considered for the stability analysis of a thin shell, the thickness has a higher significance than the others.

Elliptic paraboloid shell is commonly used doubly curved positive Gaussian curvature shell structure. So it has significant importance to determine the influence of parameters in the designing process of the shell.

Modeling and analyzing of the shell by RFEM finite element software that helps to determine the internal forces, critical buckling loads, and free vibration. The results gained from the software also have good resemble the theoretical results except for the free vibration. The buckling and natural free vibration mode shape also determined from the software.

Generally, in this study, thin shell analysis, buckling and free vibration of the elliptic parabolic shell structures are performed. First of all, the internal force, moment, and deformation in the central section and around the edge of the shell by its own weight of shell was determined by theoretical and numerical analysis. After that, the critical buckling analysis is completed by both methods. Finally, the free vibration of the shell is worked for a rectangular and square planed elliptic paraboloid shell model.

Results of the free vibration demonstrate that the theoretical result does not give the same solution to the finite element analysis this might be due to assumptions during drive a theoretical formula. From this, it has decided that this study required experimental work.

5.2 Recommendations

This thesis study only linear analysis of the shell, the structure is performed by finite element analysis therefore, it has recommended that further experimental researches should be investigated concerning linear and nonlinear analysis.
Stability of elliptical paraboloid shell under own weight with simply supported around the edge was studied in this thesis other researchers will make including all other load types acting on shells and other boundary conditions around the edge of the shell.

This study focused only on the linear analysis of reinforced concrete elliptic parabolic shell structure on specified parameters so it has recommended other researchers will make on other elliptic parabolic shells that have different dimensions and parameters.

Modeling and analysis of the elliptic parabolic shell structures are done by Dlubal RFEM finite element software. For future work, it could be also recommended that the Dlubal RFEM finite element software is used for other types of shell and other structural works.

MATLAB is useful in this thesis to write a code for theoretical double Fourier series formulas that are not easily calculated by manual hand calculations and other software therefore other researchers use this software for many purposes.

REFERENCES

[1] G. L. Gbaguidi-Aisse and S. N. Krivoshapko, "Geometry, Static, Vibration and Buckling Analysis and Applications to Thin Elliptic Paraboloid Shells," *The Open Construction and Building Technology Journal,* vol. 10, no. 229, pp. 576–602, 2016, doi: 10.2174/1874836801610010576.

[2] A. M. Ansah, "Elastic Analysis of Elliptic Paraboloids," The Ghana Academy of Science, 1967.

[3] H. Djamal, M. Mellas, and R. Chebili, "Numerical and Experimental Investigation of an Elliptical Paraboloid Shell Model," *Research Gate*, vol. 2. Proceedings of the World Congress on Engineering, London, U.K, p. 6, 2009.

[4] T. Nagy, "Some Problems of the Numerical Analysis of Elliptic Paraboloid Shallow Shells," Budapest Technical University, 1976.

[5] N. Tamboli and A. B. Kulkarni, "Bending Analysis of Paraboloid of Revolution Shell," *International Journal of Civil Engineering Research*, vol. 5, no. 4, pp. 307–314, 2014.

[6] B. Mohraz and W. C. Schnobrich, "The Analysis of Shallow Shell Structures by Discrete Element System," Urbana, 1966.

[7] S. Kato, Y. Yamauchi, T. Ueki, and K. Okuhira, "Buckling Load of Elliptic Paraboloidal Single Layer Reticulated Roofs with Simple Supports under Uniform Load," *International Journal of Space Structures*, vol. 20, no. 4, pp. 211–224, 2005.

[8] F. Ruo-Qiang, Y. Jihong, and Y. Bin, "Evaluation of the Buckling Load of an Elliptic Paraboloid Cable-Braced Grid Shell Using the Continuum Analogy," *Journal of Engineering Mechanics*, vol. 138, no. 12, pp. 1468–1478, 2012, doi: 10.1061/(ASCE)EM.1943-7889.0000454.

[9] A. Zingoni and V. Balden, "On the Buckling Strength of Stiffened Elliptic Paraboloidal Steel Panels," *ELSEVIER*, vol. 1, no. 47, pp. 661–667, 2009, doi: 10.1016/j.tws.2008.11.007.

[10] N. N. Meleka, A. A.Bashandy, M. A. Safan, and A. S. Abd-Elrazek, "Repairing and Strengthening of Elliptical Paraboloid Reinforced Concrete Shells with Openings," Menoufiya University, 2013.

[11] A. Bryan, "Free Vibration of Thin Shallow Ellipitical Shells," *ASME Journal of Vibration and Acoustics*, vol. 16, no. 1431, pp. 1–38, 2017, doi: 10.1115/1.4035958.

[12] A. N. Nayak and J. N. Bandyopadhyay, "On the Free Vibration of Stiffened Shallow Shells," *Journal of Sound and Vibration*, vol. 255, no. 2, pp. 357–382, 2002, doi: 10.1006/jsvi.2001.4159.

[13] M. Farshad, *Design and Analysis of Shell Structures*, 1st ed. Switzerland: Kluwer Academic Publishers, 1992.

[14] P. C. Varghese, *Design of Reinforced Concrete Shells and Folded Plates*, 1st ed. New Delhi: PHI Learning Private Limited, 2010.

[15] E. Ventsel and T. Krauthammer, *Thin Plates and Shells*, 10th ed. New York: Marcel Dekker, Inc., 2001.

[16] D. P. Billington, *Thin Shell Concrete Structures*, 2nd ed. New York: McGraw-HILL Publishing Company, 1990.

[17] I. Iskhakov and Y. Ribakov, "Design Principles and Analysis of Thin Concrete Shells, Domes and Folders," Taylor & Francis Group, LLC, Israel, 2016.

[18] W. Soedel, *Vibration of Shells and Plates*, 3rd ed. New York: Marcel Dekker, Inc., 2004.

[19] EBCS EN 1992-1-1, "Design of Concrete Structures Section 3 : Materials," Ministry of Urban Development and Construction, Addis Ababa, 2013.

[20] MATLAB, "MATLAB-Programming Platform Designed Specifically for Engineers and Scientists." MathWorks Inc., Natick, Massachusetts, USA, 2019.

[21] RFEM, "RFEM - A Finite Element Program For Structural Analysis and Design." Dlubal Software GmbH, Tiefenbach, Eastern Bavaria, Germany, 2016.

[22] Dlubal Software GmbH, "RF-STABILITY," 2014. [Online]. Available: http://www.dlubal.com. [Accessed: 10-Oct-2019].

[23] Dlubal Software GmbH, "RF-DYNAM Pro," 2016. [Online]. Available: http://www.dlubal.com. [Accessed: 04-Jan-2020].

APPENDIX A TABLE OF COEFFICIENT

Coefficients for computing force components in elliptical paraboloid when C_1/C_2 =1.

x/a	Parameter	*y/b*				
		0.000	0.250	0.500	0.750	1.000
0	*F1*	0.250	0.267	0.318	0.399	0.500
	F2	0.250	0.233	0.182	0.101	0.000
	F3	0.000	0.000	0.000	0.000	0.000
0.25	*F1*	0.233	0.250	0.301	0.389	0.500
	F2	0.267	0.250	0.199	0.111	0.000
	F3	0.000	0.029	0.068	0.096	0.108
0.50	*F1*	0.182	0.199	0.250	0.350	0.500
	F2	0.318	0.301	0.250	0.150	0.000
	F3	0.000	0.068	0.140	0.210	0.244
0.75	*F1*	0.101	0.111	0.150	0.250	0.500
	F2	0.399	0.389	0.350	0.250	0.000
	F3	0.000	0.096	0.210	0.356	0.465
1	*F1*	0.000	0.000	0.000	0.000	0.000
	F2	0.500	0.500	0.500	0.500	0.000
	F3	0.000	0.108	0.243	0.465	∞

Coefficients for computing force components in elliptical paraboloid when C_1/C_2 = 0.8.

x/a	Parameter	*y/b*				
		0.000	0.250	0.500	0.750	1.000
0	*F1*	0.211	0.230	0.287	0.381	0.500
	F2	0.289	0.270	0.213	0.119	0.000
	F3	0.000	0.000	0.000	0.000	0.000
0.25	*F1*	0.196	0.215	0.272	0.370	0.500
	F2	0.304	0.285	0.228	0.130	0.000
	F3	0.000	0.034	0.069	0.100	0.114
0.50	*F1*	0.153	0.169	0.223	0.331	0.500
	F2	0.347	0.331	0.277	0.169	0.000
	F3	0.000	0.065	0.139	0.215	0.255
0.75	*F1*	0.084	0.094	0.131	0.230	0.500
	F2	0.416	0.406	0.369	0.270	0.000
	F3	0.000	0.091	0.201	0.353	0.480
1	*F1*	0.000	0.000	0.000	0.000	0.000
	F2	0.500	0.500	0.500	0.500	0.000
	F3	0.000	0.101	0.229	0.443	∞

Coefficients for computing force components in elliptical paraboloid when $C_1/C_2 = 0.6$.

x/a	Parameter	*y/b*				
		0.000	0.250	0.500	0.750	1.000
0	*F1*	0.164	0.184	0.248	0.357	0.500
	F2	0.336	0.316	0.252	0.143	0.000
	F3	0.000	0.000	0.000	0.000	0.000
0.25	*F1*	0.152	0.171	0.233	0.345	0.500
	F2	0.348	0.329	0.267	0.155	0.000
	F3	0.000	0.031	0.067	0.103	0.120
0.50	*F1*	0.117	0.133	0.188	0.304	0.500
	F2	0.383	0.367	0.312	0.197	0.000
	F3	0.000	0.060	0.132	0.216	0.265
0.75	*F1*	0.084	0.094	0.131	0.230	0.500
	F2	0.436	0.426	0.392	0.296	0.000
	F3	0.000	0.081	0.185	0.342	0.494
1	*F1*	0.000	0.000	0.000	0.000	0.000
	F2	0.500	0.500	0.500	0.500	0.000
	F3	0.000	0.089	0.208	0.413	∞

Coefficients for computing force components in elliptical paraboloid when $C_1/C_2 = 0.4$

x/a	Parameter	*y/b*				
		0.000	0.250	0.500	0.750	1.000
0	*F1*	0.105	0.126	0.193	0.320	0.500
	F2	0.395	0.374	0.307	0.180	0.000
	F3	0.000	0.000	0.000	0.000	0.000
0.25	*F1*	0.097	0.117	0.181	0.308	0.500
	F2	0.403	0.383	0.319	0.192	0.000
	F3	0.000	0.026	0.060	0.101	0.125
0.50	*F1*	0.075	0.090	0.143	0.265	0.500
	F2	0.425	0.410	0.357	0.235	0.000
	F3	0.000	0.049	0.115	0.208	0.274
0.75	*F1*	0.041	0.049	0.081	0.169	0.500
	F2	0.459	0.451	0.419	0.331	0.000
	F3	0.000	0.065	0.156	0.316	0.506
1	*F1*	0.000	0.000	0.000	0.000	0.000
	F2	0.500	0.500	0.500	0.500	0.000
	F3	0.000	0.070	0.173	0.363	∞

Coefficients for computing force components in elliptical paraboloid shells when C_1/C_2 = 0.2

x/a	Parameter	*y/b*				
		0.000	0.250	0.500	0.750	1.000
0	*F1*	0.038	0.054	0.112	0.252	0.500
	F2	0.462	0.446	0.388	0.248	0.000
	F3	0.000	0.000	0.000	0.000	0.000
0.25	*F1*	0.035	0.049	0.104	0.239	0.500
	F2	0.465	0.451	0.396	0.261	0.000
	F3	0.000	0.014	0.040	0.088	0.128
0.50	*F1*	0.027	0.038	0.086	0.197	0.500
	F2	0.473	0.462	0.414	0.303	0.000
	F3	0.000	0.027	0.074	0.174	0.280
0.75	*F1*	0.015	0.020	0.044	0.117	0.500
	F2	0.485	0.480	0.456	0.383	0.000
	F3	0.000	0.034	0.098	0.246	0.510
1	*F1*	0.000	0.000	0.000	0.000	0.000
	F2	0.500	0.500	0.500	0.500	0.000
	F3	0.000	0.038	0.108	0.262	∞

Values of the dimensionless coefficient at the central point of the shell by DMV theory.

Values of the dimensionless coefficients at the central Point of the Shell			
Parameter λ	Shallow Shell		
	$\overline{\omega}$	$\overline{N}$	$\overline{M}$
0.5	36.2101	4.2401	3.7985
1.0	27.2112	6.3618	2.7911
1.5	19.2000	6.7200	1.9396
2.0	13.4115	6.2501	1.1988
3.0	7.0851	4.9501	0.5066
4.0	4.1200	3.8102	0.2106
5.0	2.6100	3.0115	0.0709
6.0	1.7511	2.4510	0.0140
10.0	0.5601	1.3102	-0.0218
20.0	0.1364	0.6201	-0.0002

APPENDIX B MATLAB CODING

```
%Addis Ababa University
%Addis Ababa Institute of Technology
%Department of Civil and Environmental Engineering
%Stream Structural Engineering
%NAME: TAMIRAT KEBEDE MITIKU
%ID: GSR/1719/10
%SUBMITED TO: AAIT Post graduate program
% Method of Table of Coefficient
a = input('  Enter the value of a in meter :\n');
% a is Plan dimension in x direction
b = input('  Enter the value of b in meter :\n');
% b is Plan dimension in y direction
h1 = input('  Enter the value of h1 in meter :\n');
% h1 is rise of shell in short direction
h2 = input('  Enter the value of h2 in meter :\n');
% h2 is rise of shell in long direction
x = input('  Enter the value of x in meter :\n');
y = input('  Enter the value of y in meter :\n');
P = input('  Enter the value of P :\n')
% P is Own weight of the shell kN/m^2
q=0;
for n=1:2:360
q=q+2*((((-1)^((n-
1)/2)*cosh((n*pi*sqrt(h1/h2)/(2*a))*x)*cos((n*pi/(2*b))*y)/(pi*n*cosh((
n*pi*sqrt(h1/h2)/(2*a))*a)))));
end
F1=-sum(q-0.5)
Nx=-(P*a^2)*F1/(h1)
F2=sum(q)
Ny=-(P*b^2)*F2/(h2)
i=0;
for n=1:2:360
i=i+2*((((-1)^((n-
1)/2)*sinh((n*pi*sqrt(h1/h2)/(2*a))*x)*sin((n*pi/(2*b))*y)/(pi*n*cosh((
n*pi*sqrt(h1/h2)/(2*a))*a)))));
end
F3=sum(i)
Nxy=-(P*a*b)*F3/(sqrt(h1*h2))
%%%%%%%%%%%%%%%%%%%%%%%%%%%%%%%%%%%%%%%%%%%%%%%%%%%%%%%%%%%%%%%%%%%%%%%%%%%%
% Method 2 Donnel Mushtari vlasov (Shallow Shell Theory)
format short
E=input('  Enter the value of E  :\n');
%Elacticity of modulus kN/m^2
v= input('  Enter the value of v :\n');
% Poissones Ratio
t= input('  Enter the value of t in meter :\n');
% thickness of the shell
a= input('  Enter the value of a in meter :\n');
% a is Plan dimension in x direction
b= input('  Enter the value of b in meter :\n');
% b is Plan dimension in y direction
f1= input('  Enter the value of f1 in meter :\n');
% f1 is rise of shell in short direction
f2=  input('  Enter the value of f2 in meter :\n');
% f2 is rise of shell in long direction
x= input('  Enter the value of x in meter :\n');
y= input('  Enter the value of y in meter :\n');
```

```
P= input('  Enter the value of P :\n');
% P is Own weight of the shell kN/m^2
nx=0;
for n=1:2:1000
    for m=1:2:1000

nx=nx+(((8*b^2*E*t*(f1+(m^2*f2)/n^2)*(sin(m*pi*x/a)*sin(n*pi*y/b))*(n^2
*pi^2/b^2)/((n^2*pi^2*a^2)*((1+(m^2*b^2)/(n^2*a^2)))^2)))*(16*P*t/(pi^2
*m*n*E))*(((pi)^4*n^4*t^4/(12*(1-
v^2)*b^4)*(1+m^2*b^2/(n^2*a^2))^2+(64*t^2/(a^4*(1+m^2*b^2/(n^2*a^2))^2)
*(f1+m^2*f2/n^2)^2)))^-1);
    end
end
Nx =-sum(nx)
ny=0;
for n=1:2:1000
    for m=1:2:1000

ny=ny+(((8*b^2*E*t*(f1+(m^2*f2)/n^2)*(sin(m*pi*x/a)*sin(n*pi*y/b))*(m^2
*pi^2/a^2)/((n^2*pi^2*a^2)*((1+(m^2*b^2)/(n^2*a^2)))^2)))*(16*P*t/(pi^2
*m*n*E))*(((pi)^4*n^4*t^4/(12*(1-
v^2)*b^4)*(1+m^2*b^2/(n^2*a^2))^2+(64*t^2/(a^4*(1+m^2*b^2/(n^2*a^2))^2)
*(f1+m^2*f2/n^2)^2)))^-1);
    end
end
Ny=-sum(ny)
nxy=0;
for n=1:2:1000
    for m=1:2:1000

nxy=nxy+(((8*b^2*E*t*(f1+(m^2*f2)/n^2)*(cos(m*pi*x/a)*cos(n*pi*y/b))*(m
*n*pi^2/(a*b))/((n^2*pi^2*a^2)*((1+(m^2*b^2)/(n^2*a^2)))^2)))*(16*P*t/(
pi^2*m*n*E))*(((pi)^4*n^4*t^4/(12*(1-
v^2)*b^4)*(1+m^2*b^2/(n^2*a^2))^2+(64*t^2/(a^4*(1+m^2*b^2/(n^2*a^2))^2)
*(f1+m^2*f2/n^2)^2)))^-1);
    end
end
Nxy=-sum(nxy)
D=(E*t^3/(12*(1-v^2)))
mx=0;
for n=1:2:1000
    for m=1:2:1000
        mx=mx+(((((pi)^4*n^4*t^4/(12*(1-
v^2)*b^4)*(1+m^2*b^2/(n^2*a^2))^2+(64*t^2/(a^4*(1+m^2*b^2/(n^2*a^2))^2)
*(f1+m^2*f2/n^2)^2)))^-
1)*(16*P*t/(pi^2*m*n*E))*(sin(m*pi*x/a)*sin(n*pi*y/b))*((m^2*pi^2/a^2)+
(v*n^2*pi^2/b^2)));
    end
end
Mx=D*sum(mx)
my=0;
for n=1:2:1000
    for m=1:2:1000
        my=my+(((((pi)^4*n^4*t^4/(12*(1-
v^2)*b^4)*(1+m^2*b^2/(n^2*a^2))^2+(64*t^2/(a^4*(1+m^2*b^2/(n^2*a^2))^2)
*(f1+m^2*f2/n^2)^2)))^-
1)*(16*P*t/(pi^2*m*n*E))*(sin(m*pi*x/a)*sin(n*pi*y/b))*((n^2*pi^2/b^2)+
(v*m^2*pi^2/a^2)));
    end
end
```

```
My=D*sum(my)
mxy=0;
for n=1:2:1000
    for m=1:2:1000

mxy=mxy+((cos(m*pi*x/a)*cos(n*pi*y/b))*(16*P*t/(pi^2*m*n*E))*(m*n*pi^2/
(a*b))*(((pi)^4*n^4*t^4/(12*(1-
v^2)*b^4)*(1+m^2*b^2/(n^2*a^2))^2+(64*t^2/(a^4*(1+m^2*b^2/(n^2*a^2))^2)
*(f1+m^2*f2/n^2)^2)))^-1);
    end
end
Mxy=-D*(1-v)*sum(mxy)
w=0;
for n=1:2:1000
    for m=1:2:1000

w=w+((sin(m*pi*x/a)*sin(n*pi*y/b))*(16*P*t/(pi^2*m*n*E))*(((pi)^4*n^4*t
^4/(12*(1-
v^2)*b^4)*(1+m^2*b^2/(n^2*a^2))^2+(64*t^2/(a^4*(1+m^2*b^2/(n^2*a^2))^2)
*(f1+m^2*f2/n^2)^2)))^-1);
    end
end
W=sum(w)
%%%%%%%%%%%%%%%%%%%%%%%%%%%%%%%%%%%%%%%%%%%%%%%%%%%%%%%%%%%%%%%%%%%%%%%%%%%%
% For Critical Buckling and Natural Vibration Analysis
a=input('  Enter the value of a  :\n');
% a is Plan dimension in x direction
b=input('  Enter the value of b  :\n');
% b is Plan dimension in y direction
h=input('  Enter the value of h  :\n');
% thickness of the shell
v=input('  Enter the value of v  :\n');
% Poissones Ratio
R1=input('  Enter the value of R1  :\n');
% radius of Curvature in x direction
R2=input('  Enter the value of R2  :\n');
% radius of Curvature in y direction
k1=1/R1
% Curvature of the curve in the x direction
k2=1/R2
% Curvature of the curve in the y direction
E=input('  Enter the value of E  :\n');
%Elacticity of modulus kN/m^2
p=input('  Enter the value of P  :\n');
% own weight of the shell kN/m^2
D=(E*h^3/(12*(1-v^2)))
Pcr=(2*E*h^2)/(R1*R2*sqrt(3*(1-v^2)))
n=pi/a
m=pi/b
wmn=((1/(p*h))*((D*((n)^2+(m)^2)^2+E*h*((n)^2/R2+(m)^2/R1)^2/((n)^2+(m)
^2)^2)))
% Natural Angular Frequency
Wmn=sqrt(wmn)
% Natural Frequency
f=Wmn/(2*pi)
% Natural Period
t=1/f
```